

AD-A148 139

DOT/FAA/PM-84/13

Project Report
ATC-128

6

An Automatic Weather Station Network for Low-Altitude Wind Shear Investigations

M.M. Wolfson
J.T. DiStefano
D.L. Kingle

18 September 1984

Lincoln Laboratory

MASSACHUSETTS INSTITUTE OF TECHNOLOGY
LEXINGTON, MASSACHUSETTS



Prepared for the Federal Aviation Administration.

Document is available to the public through
the National Technical Information Service,
Springfield, Virginia 22161

NOV 3 0 1984

A

94 11 20 311

FILE NUMBER

NOTICE

This document is disseminated under the sponsorship of the Department of Transportation in the interest of information exchange. The United States Government assumes no liability for its contents or use thereof.

TECHNICAL REPORT DOCUMENTATION PAGE

1. Report No. DOT-FAA-PM-84/13	2. Government Accession No. AD-A148139	3. Recipient's Catalog No.	
4. Title and Subtitle An Automatic Weather Station Network for Low-Altitude Wind Shear Investigations		5. Report Date 18 September 1984	
6. Author(s) Marilyn M. Wolfson, John T. DiStefano, Diana L. Kingle		7. Performing Organization Code	
8. Performing Organization Name and Address Lincoln Laboratory, M.I.T. P.O. Box 73 Lexington, MA 02173-0073		9. Work Unit No.	
10. Sponsoring Agency Name and Address Department of Transportation Federal Aviation Administration Systems Research and Development Service Washington, D.C. 20591		11. Contract or Grant No. DTFA01-80-Y-10546	
12. Supplementary Notes The work reported in this document was performed at Lincoln Laboratory, a center for research operated by Massachusetts Institute of Technology, under Air Force Contract F19628-80-C-0002.		13. Type of Report and Period Covered Project Report	
14. Sponsoring Agency Code			
15. Abstract During the summer of 1983 an experimental network of automatic weather stations (a mesonet) was operated in the vicinity of Hanscom Field, northwest of Boston, as part of a larger effort to collect Doppler radar and meteorological data on thunderstorms and other potentially hazardous weather events in this area. This report describes the mesonet system used and presents in detail the data collected on 21-22 July 1983. Conclusions about the limitations and the future use of the mesonet system are also included.			
16. Key Words mesonet automatic weather station PROBE station		17. Distribution Statement Document is available to the public through the National Technical Information Service, Springfield, Virginia 22161.	
18. Security Classif. (of this report) Unclassified	19. Security Classif. (of this page) Unclassified	20. No. of Pages 68	21. Price

ACKNOWLEDGEMENTS

Many individuals were responsible for making the mesonet project a reality in a very short period of time. We wish to specially thank A. Cameron, M. Couture, N. Kinch, D. Meuse, A. Doiron, F. Groezinger, M. Merritt, D. Hamilton, E. Becotte, J. A. Misner, B. Farino, M. Dalpe' and K. Callwood of Lincoln Laboratory, K. Hardy, R. Fournier, and S. Meunch of the Air Force Geophysics Laboratory, P. Hurley, W. Harrison, B. Silverman, and P. Hajney of the Bureau of Reclamation, R. McConnell of ERT, and D. Turnbull and C. Jones of the FAA.

We also thank the Air Force Geophysics Laboratory for the satellite data published herein, and the Bureau of Reclamation for some of the software used in plotting the mesonet data.

Above all, we thank the individual landowners who, by allowing us to use their property, gave us the chance to experiment with our weather stations and gain valuable experience in their deployment and operation.



LIST OF ACRONYMS AND ABBREVIATIONS

AFGL	Air Force Geophysics Laboratory
AWS	Air Force Air Weather Service
DCP	Data Collection Platform
EDT	Eastern Daylight Time
EST	Eastern Standard Time
FAA	Federal Aviation Administration
GOES	Geostationary Operational Environmental Satellite
JAWS	Joint Airport Weather Studies
mesonet	Mesoscale network (usually of weather stations)
MIT	Massachusetts Institute of Technology
NEMA	National Electrical Manufacturers' Association
NESDIS	National Environmental Satellite, Data, and Information Service
NEXRAD	Next Generation Weather Radar
NOAA	National Oceanic and Atmospheric Administration
NWS	National Weather Service
PROBE	Portable Remote Observations of the Environment (name for automatic weather stations)

CONTENTS

Acknowledgements	iii
List of Acronyms and Abbreviations	iv
List of Figures	vii
I. INTRODUCTION	1
A. Overview of Weather Radar Studies - Summer 1983	1
B. Low Altitude Wind Shear	2
C. Scientific Objectives	4
D. Experimental Design	7
II. THE MESONET	10
A. Background	10
B. The 1983 Network	13
C. Weather Station Instrumentation	15
1. Wind Speed and Direction Sensors	16
2. Temperature and Humidity Probe	16
3. Pressure Transducer	17
4. Precipitation Gauge	17
D. Data Collection Platforms	18
E. Site Hardware	19
1. Tower	19
2. Electronics Enclosure	19
3. Solar Panels	19
4. Lightning Protection	19
III. CASE STUDY: 21 July 1983	20
A. Introduction	20
B. Summary of Weather Situation	20
C. Satellite Data	26
D. Mesonet Data	26
1. Explanation of Figures	31
2. Features of the Data	31
3. Discussion of Individual Station Data	32
E. Doppler Radar Data	48
F. Damage Reports	48
IV. CONCLUSIONS	50
A. Upgrading Mesonet Equipment	50
1. Temporal Resolution	50
2. Operational Reliability	50

CONTENTS

V. RECOMMENDATIONS	53
A. Equipment Upgrades	53
B. Future Measurements	53
REFERENCES	54
APPENDIX A Summary of Weather Events and Collected Data	55
APPENDIX B Data Requests	58

LIST OF FIGURES

1-1	Typical structure of a mature storm cell.	3
1-2	Schematic drawing of an aircraft encounter with a microburst.	5
1-3	Vertical cross-section of microburst winds at the time of PA 759 take-off from New Orleans International Airport.	6
1-4	MIT Doppler Weather Radar in Cambridge, MA.	8
1-5	University of North Dakota instrumented Cessna Citation II.	9
1-6	Lincoln Laboratory Experimental Operations Control Center.	9
2-1	PROBE automatic weather station.	11
2-2	View of PROBE station from side not shown in Fig. 2-1.	12
2-3	Summer 1983 Mesonet.	14
3-1	Surface weather map for 2100Z on 21 July 1983.	21
3-2	Surface weather map for 0000Z on 22 July 1983.	22
3-3	Surface weather map for 0300Z on 22 July 1983.	23
3-4	Station model showing symbolic form of synoptic weather code.	24
3-5	Visible satellite image for 12:30 p.m. (EDT) on 22 July 1983.	25
3-6	Visible satellite image for 11:00 a.m. (EDT) on 21 July 1983.	27
3-7	Visible satellite image for 11:30 a.m. (EDT) on 21 July 1983.	27
3-8	Visible satellite image for 12 Noon (EDT) on 21 July 1983.	27
3-9	Visible satellite image for 12:30 p.m. (EDT) on 21 July 1983.	28

LIST OF FIGURES (Continued)

visible satellite image for 1:00 p.m. (EDT) on 21 July 1983.	28	
visible satellite image for 1:30 p.m. (EDT) on 21 July 1983.	28	45
visible satellite image for 2:00 p.m. (EDT) on 21 July 1983.	29	46
visible satellite image for 2:30 p.m. (EDT) on 21 July 1983.	29	47
visible satellite image for 3:00 p.m. (EDT) on 21 July 1983.	29	49
visible satellite image for 3:30 p.m. (EDT) on 21 July 1983.	30	49
visible satellite image for 4:00 p.m. (EDT) on 21 July 1983.	30	data 51
visible satellite image for 4:30 p.m. (EDT) on 21 July 1983.	30	
Map of weather stations (for mesonet) showing relative locations and 3-letter identifying names.	34	
Mesonet data - APC	35	
Mesonet data - LAW	36	
Mesonet data - CON	37	
Mesonet data - DUD	38	
Mesonet data - VER	39	
Mesonet data - NUB	40	
Mesonet data - NAG	41	
Mesonet data - JWL	42	
Mesonet data - PIG	43	
Mesonet data - VAL	44	

I. INTRODUCTION

A. Overview of Weather Radar Studies - Summer 1983

The Lincoln Laboratory Group 47 FAA Weather Radar Project has been concerned with identifying and understanding the technical issues associated with unique FAA needs for weather information used by pilots, air traffic controllers and meteorologists. The weather radar is a primary source of this information, but the radars currently in use have a number of deficiencies. The FAA, the National Weather Service (NWS), and the Air Force Air Weather Service (AWS) have joined together to fund a national network of "next generation" weather radars (NEXRAD) that will have advanced capabilities. In particular, the radars will be capable of sensing wind speed and direction by Doppler processing. These Doppler radars can detect rain, hail, turbulence, and low altitude wind shear and can measure the wind characteristics as a function of altitude.

However, without an expert to interpret the raw Doppler weather radar data the pilots and controllers would be unable to spot the hazards. Thus the FAA will require an automated system of weather hazard detection based on Doppler radar data. They further require that the detection be performed in real time and that the warnings be free of false alarms and be issued in a timely manner.

During the summer of 1983, Lincoln began a long term study that places emphasis on automated hazardous weather detection in the airport terminal area with a NEXRAD-like Doppler weather radar. Most fatal aircraft accidents for which weather has been cited as the cause have occurred in the airport terminal area. From investigations of these accidents it has been determined that low altitude wind shear specifically has often been the cause. Understandably, the FAA is especially interested in knowing more about the causes and the characteristics of low altitude wind shear. Thus, the Lincoln Doppler radar studies of aviation-hazardous weather focus on the automatic detection and warning of low altitude wind shear in an airport terminal area.

It is this focus on low altitude wind shear that lead us to realize that a network of automatic weather stations (the "mesonet") would be required to gather surface meteorological data in conjunction with our collection of Doppler weather radar data. The reasons for this are reviewed in section D of this chapter, on Experimental Design. A full understanding of the experiment requires that the reader have some knowledge of exactly what is meant by low altitude wind shear (this is presented in the following section) and some knowledge of our overall scientific objectives and goals (section C) as well.

Details on the mesonet system are presented in the second chapter of this report which includes information on the Summer 1983 network, the sensors used to measure the meteorological variables, and how the data is collected and processed. Although the summer of 1983 was very calm and dry in the Boston area, a data set was collected on 21 July that consisted of much rain and some hazardous weather. A case study of that day is presented in Chapter III. Finally, conclusions about the use of our weather station equipment are presented in Chapter IV, and some of our future plans are presented in Chapter V.

B. Low Altitude Wind Shear

Low altitude wind shear, in its various forms, has long been known as a hazard to aviation for it influences aircraft at probably the most vulnerable time during their entire flight. The wind shear encountered on take-off or landing has caused several tragic accidents, the most recent being the Pan Am 759 crash in July 1982 just outside of the New Orleans International Airport.

Low altitude wind shear is a broad category encompassing several distinct meteorological phenomena. The most common of these is the "gust front", the boundary between cool air flowing out from beneath a mature thunderstorm and the surrounding warm environmental air. Although a gust front is created by a particular storm cell, it can propagate miles away from the parent cell and can last for hours, as well as merge and mix with outflow currents from other neighboring cells.

The main danger for aircraft encountering a gust front is the sudden change in both horizontal and vertical wind speed and direction across the front. Since the shear zone associated with the gust front is spatially large in the along-front direction (10 km or more), is fairly persistent (lifetimes greater than 20 min), and is advected horizontally in the low level flow, the task of automatically predicting gust fronts will be manageable as long as they can be detected some distance away from the airport. Figure i-1 shows the structure of a mature thunderstorm with an overlay showing a typical aircraft glideslope penetrating the shear zone associated with the gust front.

A more recently discovered, but possibly also common meteorological phenomenon contributing to low level wind shear is the "downburst". The downburst is defined as a divergent outflow of damaging wind (>18 meters per second, 35 nautical miles per hour) of spatial extent greater than 4 km across. If the outflow is less than 4 km across, it is called a "microburst". Although downbursts and microbursts are the result of downdrafts of various sizes impacting the ground and spreading, the explanations for the downdrafts themselves differ.

**TYPICAL STRUCTURE OF A SEVERE
THUNDERSTORM CELL IN THE MATURE STAGE**

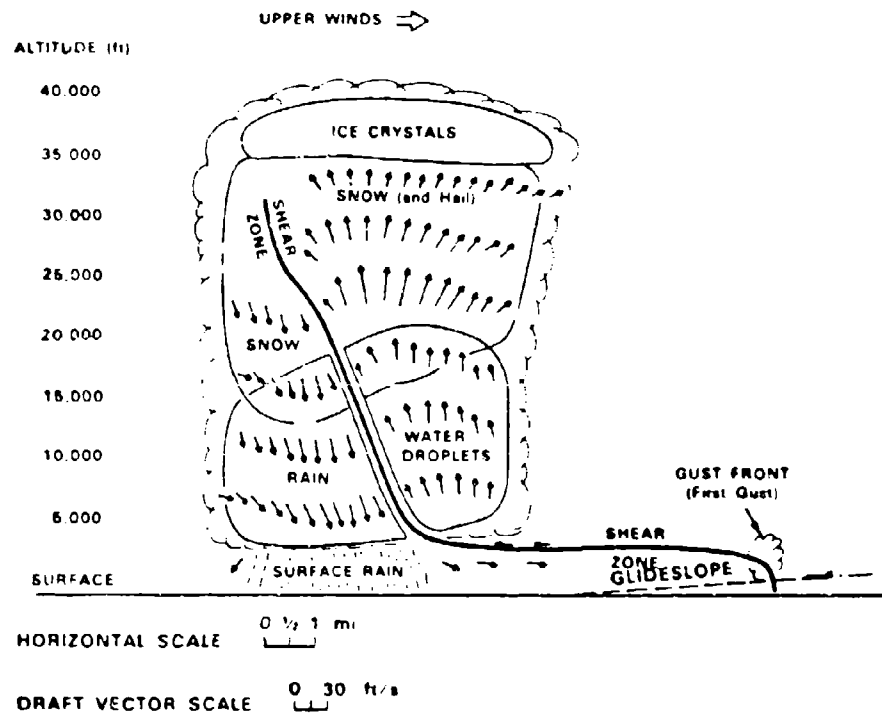


Fig. 1-1: Typical structure of a mature storm cell. The solid line, separating updraft from downdraft inside the cell and outflow from inflow in front of the cell, represents the turbulent shear zone.

The downburst or microburst, unlike the gust front, is a small scale highly divergent wind shear event. The temporal scale of a microburst can be characterized by the time from initial low altitude divergence to the time of maximum velocity differential. Wilson and Roberts (1) have shown this time scale to be approximately 4 minutes, which is in agreement with individual analyses done by Fujita (2). However, the peak outflow winds may last only one minute and be 25% to 50% stronger than those in the preceding or following minute. These features, compounded with the fact that downbursts descend from aloft rather than propagate horizontally into an area, will make them extremely difficult to predict and detect.

The downburst/microburst is truly an aircraft hazard; a plane may experience increased lift when first encountering the downburst outflow but the central downdraft and increased tailwind on the far side force the aircraft to lose airspeed and sink rapidly. Figure 1-2 illustrates the danger of an aircraft encounter with a microburst. An analysis of the Pan Am Flight 759 accident revealed that a microburst was responsible for the wind shear that caused the plane to crash. Figure 1-3 shows a vertical cross section of the low altitude winds at the time that accident took place (3).

Other sources of low altitude wind shear are squall lines, cold fronts, low level jet streams, tornadoes, and any strong localized convection which produces gusty winds and low altitude turbulence. Of all of these phenomena, the tornado is by far the most devastating. In our wind shear studies the emphasis is placed on downbursts and microbursts for they appear to be common (at least near Denver and Chicago), are not well understood, and may be the most aviation-hazardous form of low altitude wind shear.

C. Scientific Objectives

The ultimate goal of our studies is the achievement of an automated operational capability of low altitude wind shear detection and prediction in the airport terminal environment. Other data gathering experiments have shown that downbursts/microbursts are indeed a real problem and that the Doppler radar is a useful tool for detecting them. However, we need to determine the applicability of those conclusions to weather in various geographical locations.

As a first step in meeting our objective, the Lincoln Laboratory FAA Weather Radar Project conducted a small field experiment during the summer of 1983 to gather data on low altitude wind shear and downbursts associated with convective storms in the Boston area. The experiment, based in the area north and west of Boston around Hanscom Field, did provide some indication of the low altitude wind shear frequency in this area, even though the summer was unusually storm free. The main reason for conducting the experiment here was not the severity of the storms or the frequency of low altitude wind shear in this area. The reasons were:

1. because we had access to the MIT radar, and could adapt a signal processor capable of estimating Doppler velocity and filtering ground clutter to the radar fairly easily, and

AIRCRAFT ENCOUNTER WITH A MICROBURST

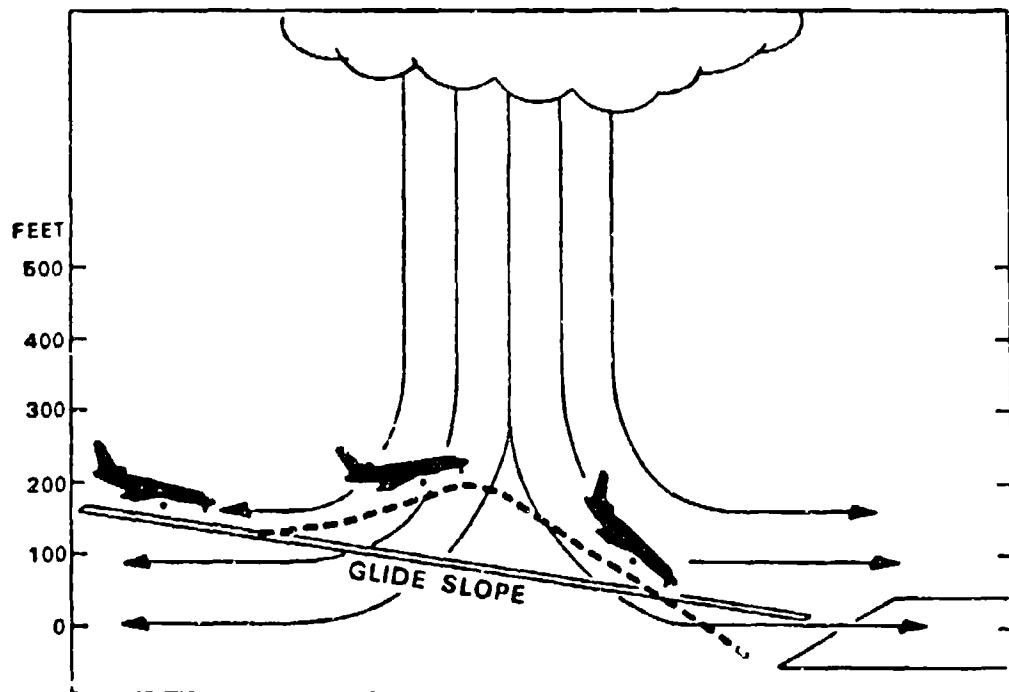


Fig. 1-2: Schematic drawing of an aircraft encounter with a microburst. Notice how the increased headwind lifts the plane above its intended glideslope while the increased tailwind causes the plane to fall below its intended glideslope.

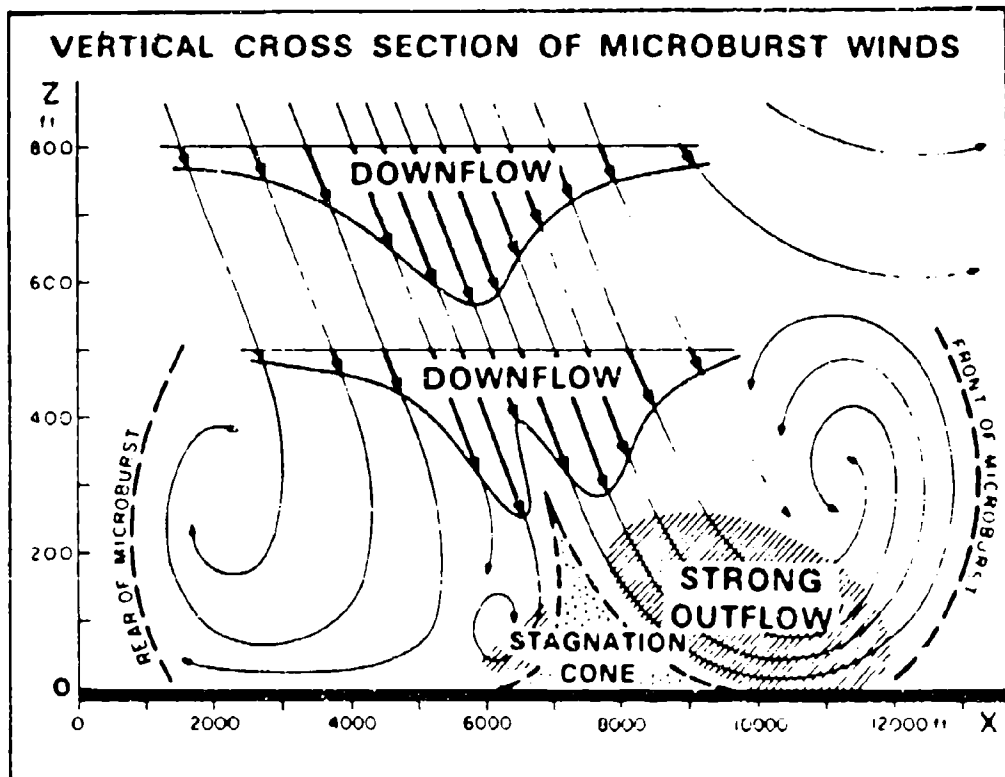


Fig. 1-3: Vertical cross section of microburst winds at the time of PA 759 take off from New Orleans International Airport. The downflow combined with the strong outflow caused the plane to lose lift and crash in a residential neighborhood near the airport. After Fujita (3).

2. to allow us to examine the degree to which a Doppler radar could collect data for use in automatic detection algorithms in the challenging ground clutter environment typical of many east coast airports.

Additionally, our experiment last summer served primarily as preparation for the use of an FAA transportable Doppler weather radar testbed now being developed at Lincoln. Upon completion (June, 1984), the testbed will be taken to its first field site in the Memphis, TN area (Olive Branch, Mississippi) where the thunderstorm frequency is expected to be very high. Subsequently, the testbed will be used to collect storm data under varying geographic and meteorological conditions.

D. Experimental Design

The Weather Radar Project collected meteorological and radar data in the Boston area during the months of July and August, 1983. Simultaneous measurements were made by the MIT S-band Doppler radar located atop the Green Building on the MIT Campus in Cambridge (Fig. 1-4), the University of North Dakota instrumented Citation II research aircraft (Fig. 1-5), and a dense array of 25 automatic surface weather stations (average spacing of 3 km) located in the area around Hanscom Field. It is this array we call a "mesonet" which is short for "mesoscale network" of weather stations.

The primary objective of operating a mesonet of automatic weather stations in conjunction with the testbed are:

1. to provide confirmation and quantification of low altitude wind shear events detected in the Doppler radar data (which detects only the radial (relative to the radar) component of the wind), and
2. to provide an indication of otherwise undetected wind shear events.

The hope is that with this mesonet data we can quantify the relationship between known wind shear events and their signatures in the radar fields. This is an essential step in development of automatic wind shear hazard detection techniques based on single Doppler radar data.

Our experimental operations control center was located at Lincoln Laboratory, where we had real-time displays of reflectivity, Doppler velocity, and turbulence (derived from the width of the Doppler spectrum) from the MIT radar, and aircraft location on an air traffic controller's plan view display (see Fig. 1-6).

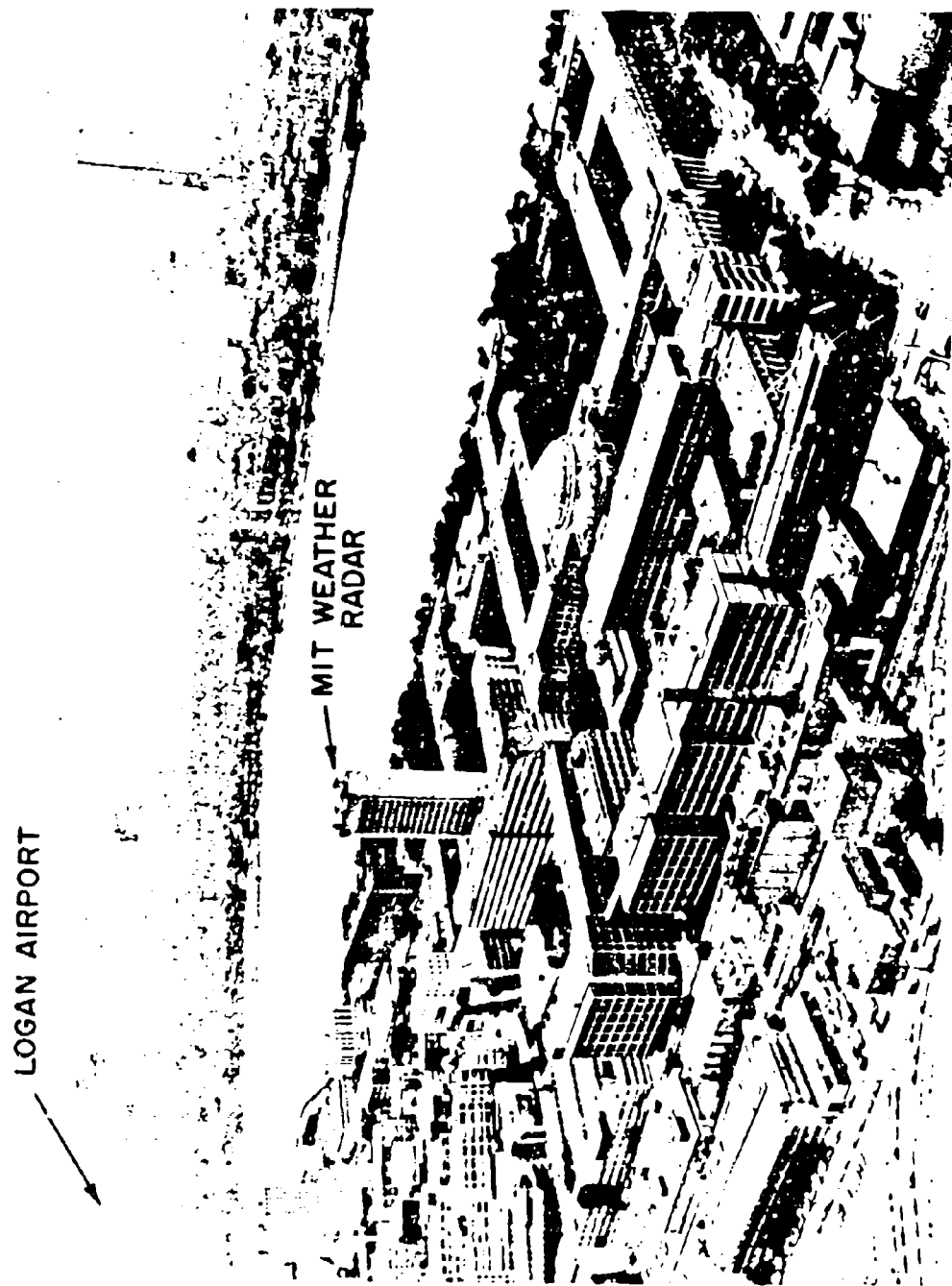


FIG. 1-4: Massachusetts Institute of Technology Doppler Weather Radar
atop the Green building on MIT campus in Cambridge, MA.

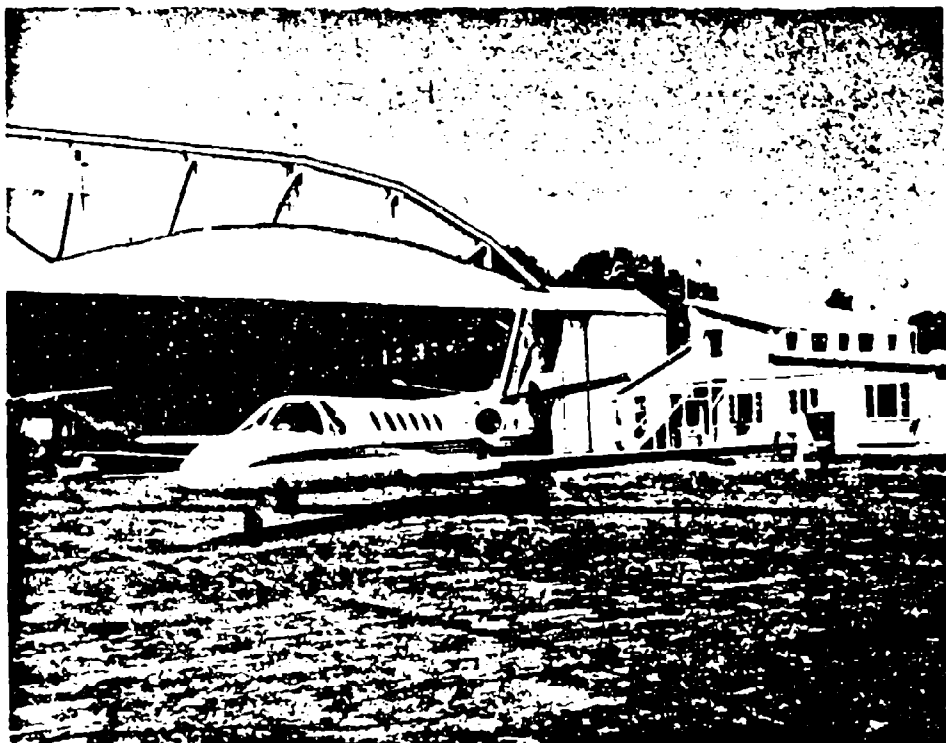


Fig. 1-5: University of North Dakota instrumented Cessna Citation II jet, parked in front of the Lincoln Laboratory Flight Facility.

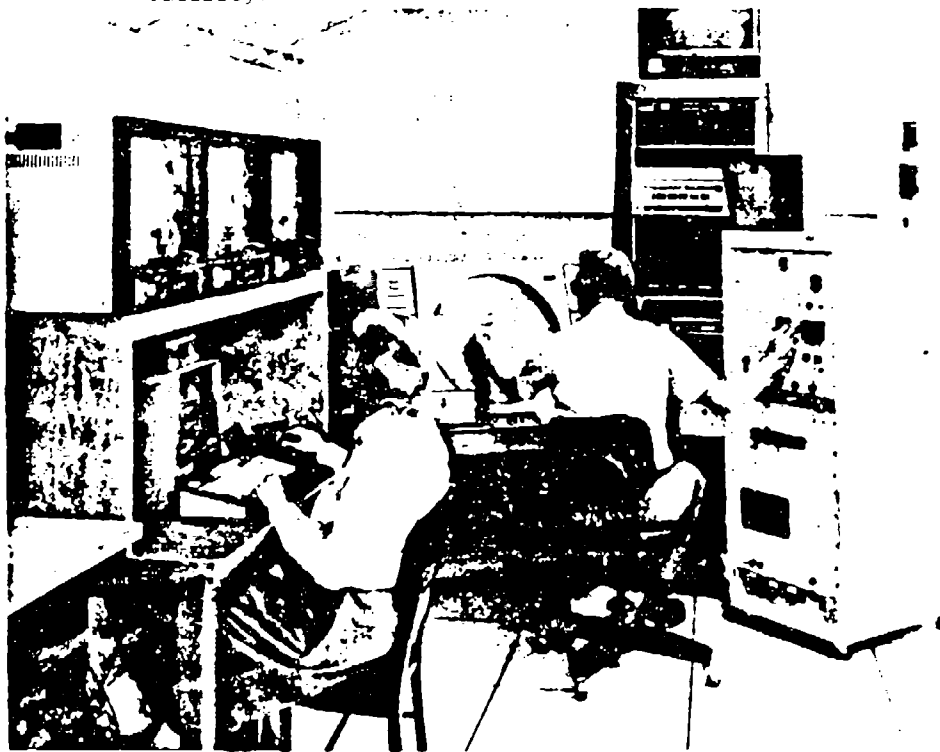


Fig. 1-6: Lincoln Laboratory Experimental Operations Control Center in Annex II. Radar data is being displayed on three monitors and radio operator is pinpointing aircraft on air traffic controller's plan view display.

II. THE MESONET

A. Background

The automatic weather stations that were first used by Lincoln Laboratory in the summer of 1983 were developed by the US Department of the Interior Bureau of Reclamation's Office of Atmospheric Resources Management in the late 1970's. These stations were given the name PROBE, standing for Portable Remote Observations of the Environment - exactly what they were designed to provide. There was a basic research need at that time for a meteorological data collection network that would allow short term predictions of convective activity, could provide good time resolution, and could be operational in very little time without the need for installing power or telephone data lines.

The stations, shown in Figs. 2-1 and 2-2, were designed to record the following surface meteorological data: temperature, relative humidity, barometric pressure, wind speed, wind direction, and precipitation amounts. Each station averages its data according to the selected interval (2 to 5 min), stores the averaged data in memory, and transmits the data at regularly timed intervals to the GOES (Geostationary Operational Environmental Satellite). The data is relayed by the satellite back to earth where it is collected by the NOAA National Environmental Satellite, Data, and Information Service's (NESDIS's) ground station on Wallops Island and by anyone with a receiving station tuned to the correct channel. An additional advantage to collecting the data this way is that the sites almost never have to be visited if they are working properly. The power for the stations is provided by a 12V deep cycle battery which is continuously trickle-charged during daylight hours by the solar panels.

The FAA arranged for the Bureau of Reclamation to furnish 25 of these PROBE stations to Lincoln Laboratory to be operated in the vicinity of Hanscom Field in support of our Summer 1983 Doppler radar experiments. The go-ahead to transfer the equipment was granted in late May and the equipment was received by Lincoln in mid-June. Sites were selected and land-owners were contacted for permission to use their open fields.

Unfortunately, a number of problems such as a delay in the allocation of a channel on the GOES EAST satellite, the failure to record data within 24 hours of its reception (the data was then lost), equipment problems and of course, inexperience all prevented the data from being continuously recorded until well into July. Even then, we had far too many problems with the equipment (some of which are illustrated in the 21 July case study) to consider the data collection successful. We did, however, achieve one of our primary objectives which was to learn what would be needed in order to successfully collect data in 1984!

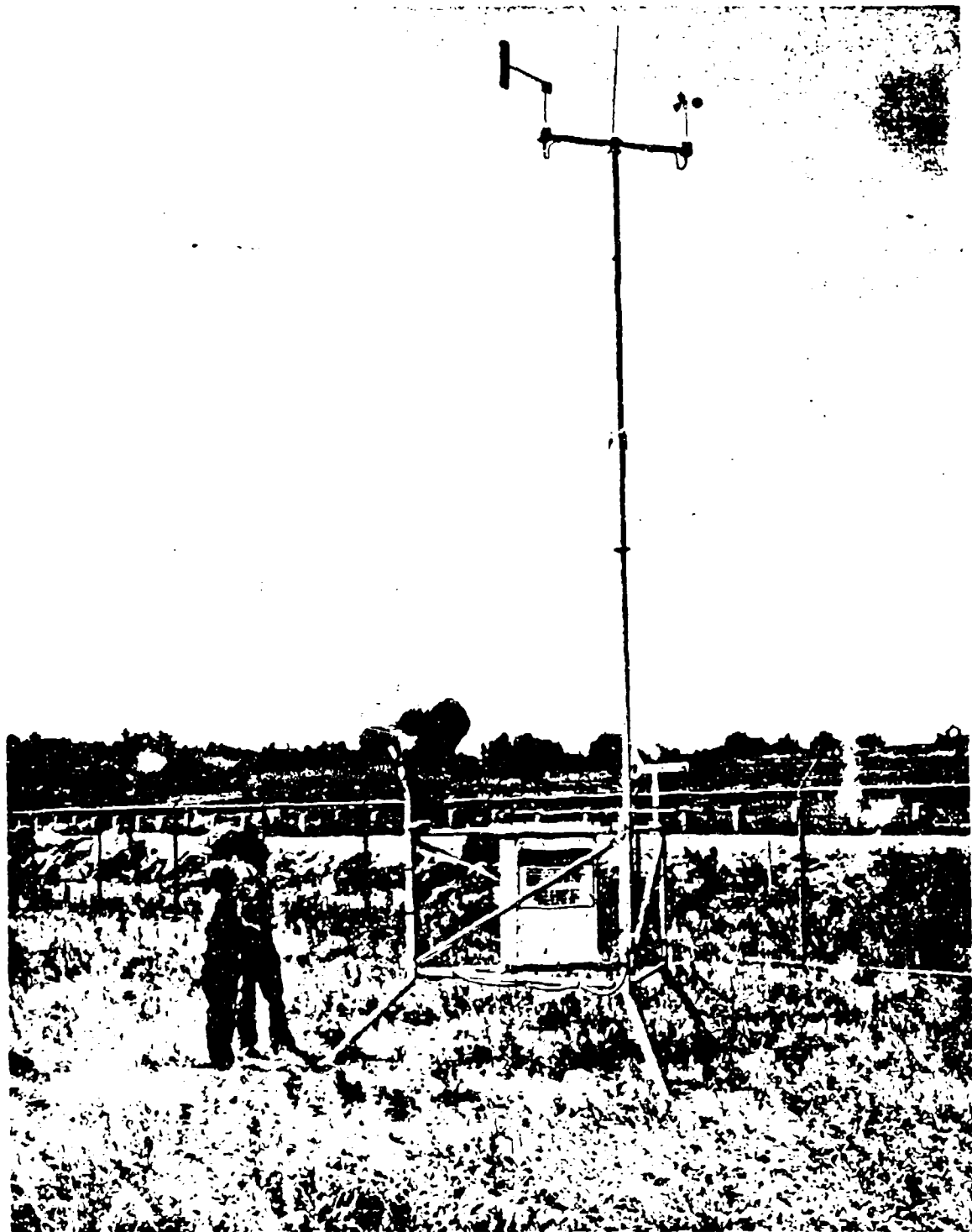


Fig. 2-2: View of PROBE station from side not shown in figure 2-1.
Technician is working on antenna. Notice wind sensor mast
is self-guyed.

B. The 1983 Network

There were three main reasons for locating the 1983 network of automatic weather stations in the vicinity of Hanscom Field. First, it would have been difficult to locate sites for the stations in the densely populated areas closer to the radar and Logan International Airport. Second, our research aircraft (from the University of North Dakota) was based at the Lincoln Laboratory Flight Facility on Hanscom Field and, due to air traffic considerations, flew experiments mainly between Gardner, MA, Hanscom, MA, and Manchester, NH. Third, the frequency of thunderstorms is greater inland than near the coast so the chances for measuring low altitude wind shear should be somewhat better.

Once the general area was decided upon, care had to be taken in choosing the individual sites. In order for an area to qualify as an acceptable site, a number of characteristics had to be considered. The weather station was placed in 4 to 5 acre open fields (pasture or crop) when possible. This size insured adequate exposure to wind and precipitation and reduced the influence of nearby buildings and trees on the measurements. Orography was another consideration in site selection. Valleys, hillsides and nearby lakes and swamps could produce microscale effects on the local weather, causing stations to report data that would not be representative of the mesoscale environment. We tried to find fields that had limited access to the public in order to guard against vandalism, but that left the nearby roads necessary for work crews to erect and maintain the stations.

The network finally selected for the Hanscom Field area is depicted in Fig. 2-3. Although there is a fair amount of unusable wooded and park land, with the help of many kind and generous landowners we were able to situate the stations in a fairly regularly spaced grid.

The station spacing was determined by the size and scale of the low altitude wind shear that we were hoping to measure. The horizontal scale of a microburst is initially less than 4 km across. Thus, we tried to site the stations approximately 3 km apart, with a maximum allowable distance of 5 km. It is sometimes difficult to justify siting the stations this close together for if they were farther apart the total network could cover a much larger area and the probability of measuring a low altitude wind shear event would be greater. However, with that approach the low resolution data collected would not reveal important features of the wind shear and would therefore be of doubtful value.

Note that there is an unusually dense network of stations around Hanscom Field. The research aircraft that we operated was able to measure wind speed and direction along its flight path. We placed weather stations at both ends of the long runway so that when the plane came in for a low approach over the airport, we would have wind measurements both at the surface and aloft.

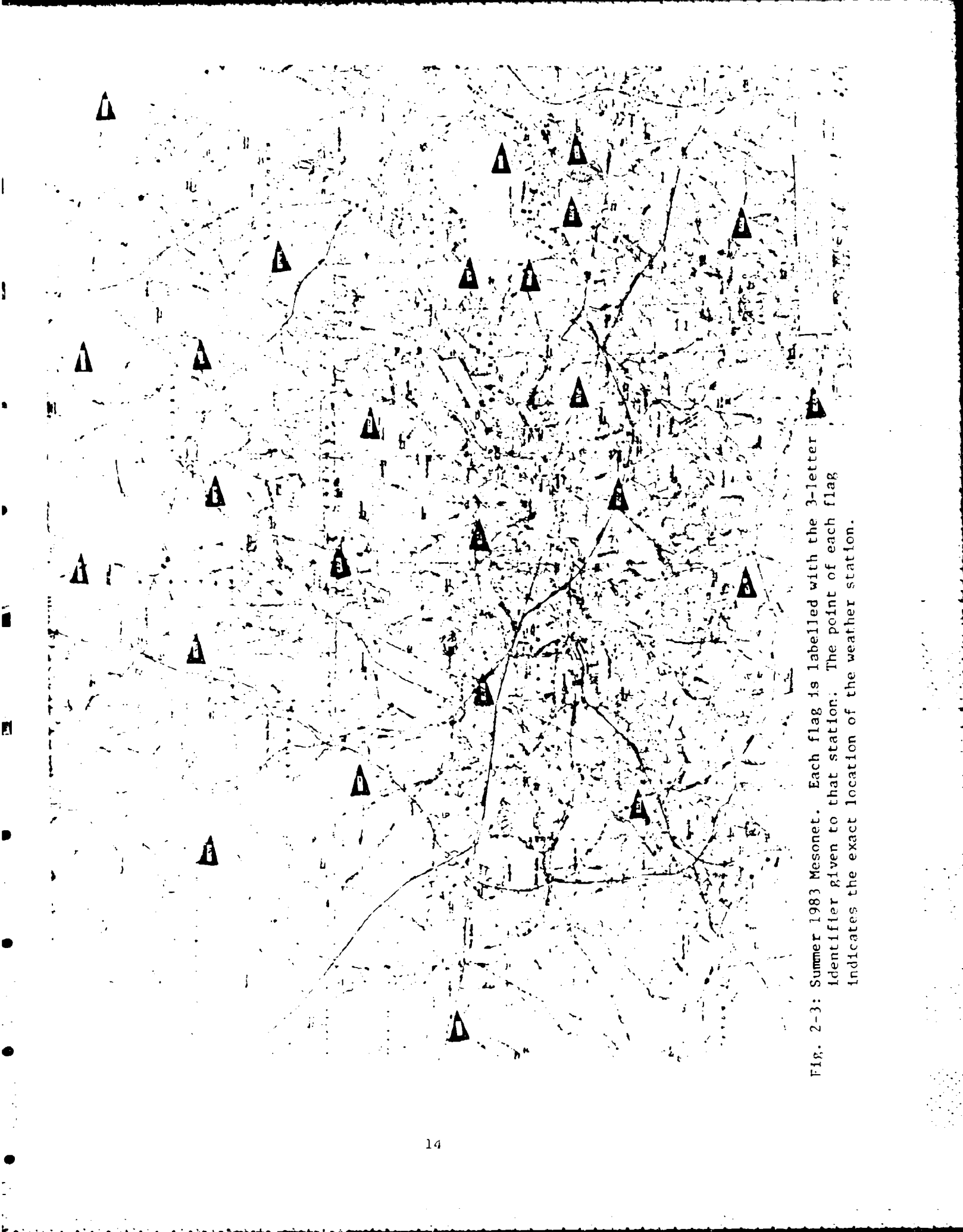


FIG. 2-3: Summer 1983 Mesonet. Each flag is labelled with the 3-letter identifier given to that station. The point of each flag indicates the exact location of the weather station.

C. Weather Station Instrumentation

The PROBE weather stations, designed by the Bureau of Reclamation are equipped to measure temperature, relative humidity, pressure, wind speed, wind direction, and precipitation amounts. The sensors were purchased from various manufacturers and, with the exception of the barometer, were used without modification. The standard station is equipped with the following sensors:

Wind Speed and Direction Meteorological Research, Inc. (MRI) model with sine-cosine output

Speed: Range: 0.2 to 54. m/s
Resolution: 0.05 m/s
Direction: Range: 0 to 360 degrees
Accuracy: 2.5 degrees
Resolution: 0.4 degrees

Temperature and Humidity Weathertronics model 5121-99

Temperature: Range: -30 to +50 degrees C
Accuracy: 0.2 degrees C
Resolution: 0.1 degree C

Humidity: Range: 0 to 100 percent
Accuracy: 3 percent
Resolution: 2 percent

Pressure Weathertronics model 7115
modified for temperature regulation

Range: 200 millibars
Resolution: 0.1 millibar

Precipitation Belfort Instrument Co. model 5915R
(weighing gauge)

Range: 0 to 300 millimeters
Resolution: 0.3 mm

Each sensor is described briefly in the following sections. The complete mechanical and electrical specifications for the sensors are available in the individual owner's manuals and have not been reproduced in this report.

1. Wind Speed and Direction Sensors

The PROBE stations are equipped with the MRI model 1022 wind speed and direction sensors. The instrument set consists of a cup and vane sensor arrangement using a common cross arm for mounting. The cross arm is attached to the top of the mast with a "T" mounting bracket equipped with set screws. The cross arm height on the PROBE station is 6.8 meters above ground level. (See Fig. 2-2.)

The sensor housing consists of a long tapered upper column, an inner cap keyed lower section and a mounting insert all made of die-cast aluminum. The sensor housings are held in place on the cross arm with hex-key set screws. The anemometer cups and the direction vane are also held with hex-key set screws.

Wind speed is derived from a photo chopper disk assembly attached to the lower end of the anemometer shaft. As the cups turn, the chopper disk breaks the light beam from a light emitting diode exactly 100 times per revolution. The output signal is a sine wave that has the same frequency as these light pulses. This frequency is directly proportional to the wind speed.

The wind direction transducer is a sine/cosine potentiometer which provides the vector components of the wind direction (cosine signal provides a voltage proportional to the east-west component and the sine signal, the north-south component). The sine/cosine potentiometer eliminates the ambiguity that can arise from averaging the wind direction over time with a straight 0-360 degree potentiometer. For example, if the wind were coming from 358 degrees half the time and from 2 degrees half the time, a 0-360 pot average would indicate a direction of 180 degrees, exactly opposite the actual average wind direction.

2. Temperature and Humidity Probe

The temperature and relative humidity probe is packaged by Weathertronics, and contains the Vaisala Humicap relative humidity sensor and the Yellow Springs Instrument (YSI) temperature sensor.

The Humicap sensing element is a thin film capacitive sensor. A very thin (1 micron) dielectric polymer layer absorbs water molecules that readily pass through a thin metal electrode causing a change in capacitance as a function of relative humidity. This function is essentially linear and independent of temperature. A solid state electronic circuit located in the probe body provides the voltage output directly proportional to percent relative humidity, over the range from 0 to 100 percent.

The temperature sensor is a YSI two element precision thermistor. Circuitry is provided in the probe for an output voltage inversely proportional to temperature. Temperature measurements are accurate over the range from -30 to +50 degrees C.

The temperature and relative humidity probe is situated on one corner of the PROBE station inside a vane aspirator (Fig. 2-1, left corner). The vane aspirator shields the probe from direct sunlight. It is painted white to reflect the sun and keep the air inside from heating up, and has a fin to keep the open end of the tube pointed into the wind. This insures a good airflow over the sensors at all times (particularly important for the thermistor).

3. Pressure Transducer

The pressure sensors used in the PROBE stations are a modified version of the Weathertronics 7115 strain gage bridge pressure transducer. The strain gage bridge has a good linear response with pressure and wears very well because it has no moving parts. Its one main drawback is the strong dependence of output on temperature.

The electronics company that developed the data collection package for the Bureau of Reclamation chose to keep the barometer at a constant temperature of 95°F as a method of temperature compensation. This was accomplished by installing a heater next to the strain gage, wrapping the package in insulating foam, putting that package inside a thermos bottle and placing the thermos inside a large styrofoam cylinder. A thermostat was put in line with the heater so that the temperature would not rise above 95°F. One of the problems with this system is the excess power it needs to keep the barometers warm. However, once the sensor has reached a constant temperature, the power used to keep it warm is minimal.

The barometer is located inside the large white armored box hanging on one side of the station triangle (see Figs. 2-1 and 2-2). This box effectively shields the barometer from the wind, which is a source of dynamic pressure fluctuations.

4. Precipitation Gauge

The precipitation gauges that were chosen for use with the weather stations are the "weighing bucket" type. These do not have the high resolution of, for example, the "tipping bucket" variety but they can measure rainfall accurately to within one-tenth of a millimeter. The gauge is simply a calibrated weighing scale on which a bucket sits. Whatever falls into the bucket will get weighed as if it were rain. For that reason and also because of evaporation, precipitation amount differences are used to determine rainfall within a given period of time.

Most of the stations in our summer 1983 network were deployed without rain gauges because the equipment was not available in time.

D. Data Collection Platforms

The data from the meteorological sensors consists of analog voltage signals or, in the case of wind speed, of frequency outputs which need to be averaged and stored for transmission. The Bureau of Reclamation had a electronic sensor interface built to perform this task. The sensor interface is connected to the Data Collection Platform which reads the data and formats it for transmission at user-specified intervals.

The electronic sensor interface is of modular design with a "mother" board and seven individual "daughter" boards, one for each sensor. The daughter boards provide the signal conditioning and digital averaging for the specified period. All daughter boards are connected to the motherboard which provides the operating and regulating voltages for the sensors and signal conditioners.

The Data Collection Platform (DCP) is a microprocessor based environmental data collection system. The user specifies which measurements are to be made and the time intervals between data collection cycles. The data are collected from the mother board, reformatted according to the required transmission protocol, and transmitted to one of the geostationary satellites (we used the GOES-EAST). The transmissions occur at regularly spaced intervals agreed upon by the satellite's controlling agency (NOAA).

There are two limitations on the averaging period selectable with the DCP. First, the design of this equipment forces 22 seconds of dead time out of every averaging period to allow the DCP to read the data from memory on the motherboard. This interruption in data sampling is acceptable with the five minute averaging period for which the equipment was originally designed, but with a one minute averaging period the system would be collecting data just over half the time.

The second limitation on the averaging period is that the DCP must be programmed with integer-minute averaging periods while the averaging period on the motherboard is a multiple (by a power of 2) of the basic five minute averaging period. There is no suitable match between the motherboard and the DCP for averaging periods less than two minutes. We chose a 3 minute averaging period on the DCP and a 2.5 minute period on the motherboard for our implementation. Taking into consideration the 22 seconds of dead time, we had only an 8 second discrepancy with this arrangement.

The Data Collection Platform used was the Handar Model 500. The DCP is housed in a cylindrical environmentally sealed can. Electrical connections are made by multipin connectors on the outside of the can. The DCP is programmable with the use of a special programming set which itself is microprocessor based. The user can program the number of data channels, the data scan times, the data transmission times, and the mode of data collection.

E. Site Hardware

The site hardware consists of the tower and tripod, the electronics enclosure and armored shielding, the solar panels and battery, and a lightning kit. Each part is described briefly in the following sections.

1. Tower

The tower consists of the Synergetics Model 1 tripod with a crossarm for wind sensor mounting at the top of the mast. The tower is a self-guyed, free standing structure capable of withstanding 50 m/s winds and limiting the mast whip to less than ± 5 cm. The mast tips down to allow easy access to the wind sensors and lightning rod. The structure easily supports up to 200 kg and has adjustable legs to provide leveling on uneven terrain. The large foot pads reduce the footprint loading of the tower itself to less than 75 g/cm². The station is shown in Figs. 2-1 and 2-2.

2. Electronics Enclosure

The station has an environmental enclosure meeting Type 12 specifications. The DCP and the sensor interface electronics are mounted within the NEMA enclosure.

The NEMA enclosure is itself surrounded by nearly 3/8 inches of steel plate. This armor is configured in two half-boxes which become part of the mounting bracket for the environmental enclosure. This white armor box completely surrounds the environmental enclosure (See Figs. 2-1 and 2-2.)

3. Solar Panels

The solar panels are mounted on the south side of the tripod and are set at a favorable angle for receiving the sun's rays. Two ARCO model 16-1200 panels are used per station. These panels each contain 36 three-inch single-crystal silicon cells enclosed in a fully weather proof assembly with a rigid, self-supporting frame. The power output is an average of 1.2 amperes at 16.2 volts DC. With two panels in parallel the peak power provided is nearly 40 watts.

The battery used is a Delco model 1150 heavy duty maintenance free battery designed for cycling applications. The battery provides 105 amp-hour capacity which could power a typical station for at least two weeks without charging. The battery is trickle-charged continuously by the output from the solar panels.

4. Lightning Protection

The lightning protection kit consists of an aluminum rod, ground wire, ground rod, cable clamps and mounting hardware. The lightning rod can be seen in Figs. 2-1 and 2-2 between the anemometer and wind vane at the top of the wind sensor mast.

III. CASE STUDY: 21 JULY 1983

A. Introduction

Our intent when we initially set up our network of weather stations was to provide each landowner with a record of the data collected by the station on their property. However, analysis showed that a substantial fraction of the total data set was flawed by electronics malfunctions, recorder failures, etc. Thus, tabulation and publication of the full mesonet results would not be appropriate.

We have decided instead to illustrate some of these problems and the utility of the mesonet data by presenting the data collected during a 48 hour period, beginning on 21 July 1983, in which severe thunderstorms broke out in our area. Along with the mesonet data, we present surface synoptic data, satellite data, and radar data. This additional data is meant to serve both as an aid in understanding the general weather situation and as an example of the different types of data that are readily available for detecting and predicting potentially hazardous weather.

We have omitted the radar Doppler velocity and spectrum width fields for this case because their interpretation is not simple and a suitable explanation is beyond the scope of this work. However, Doppler radar data is available for the 21 July case and others as well. The data collected during the summer of 1983 is summarized in Appendix A. All of this data is available to anyone interested, and the procedure for requesting it is detailed in Appendix B.

B. Summary of Weather Situation

Upper level charts at 1200 GMT (8:00 AM (EDT)) on July 21, 1983 revealed an intensifying trough of low pressure approaching New England from the northwest. Strong cyclonic vorticity advection was evident in advance of this trough. This, combined with warm advection ahead of an approaching cold front at the surface and moisture which was available at low- and mid-levels in the atmosphere, set the stage for strong thunderstorm development by late in the afternoon in most of New England.

The cold front came through southern and eastern New England during the evening hours of the 21st. Figures 3-1, 3-2 and 3-3 show the progression of this cold front as it swept southeastward through our area. Figure 3-4 gives an explanation of the station model which appears at each observation point on the surface weather maps in the three previous figures. After the front's passage, a strong surface low developed offshore on the following day (July 22, 1983). The circulation from this system was quite in evidence as shown in Figure 3-5. This storm was

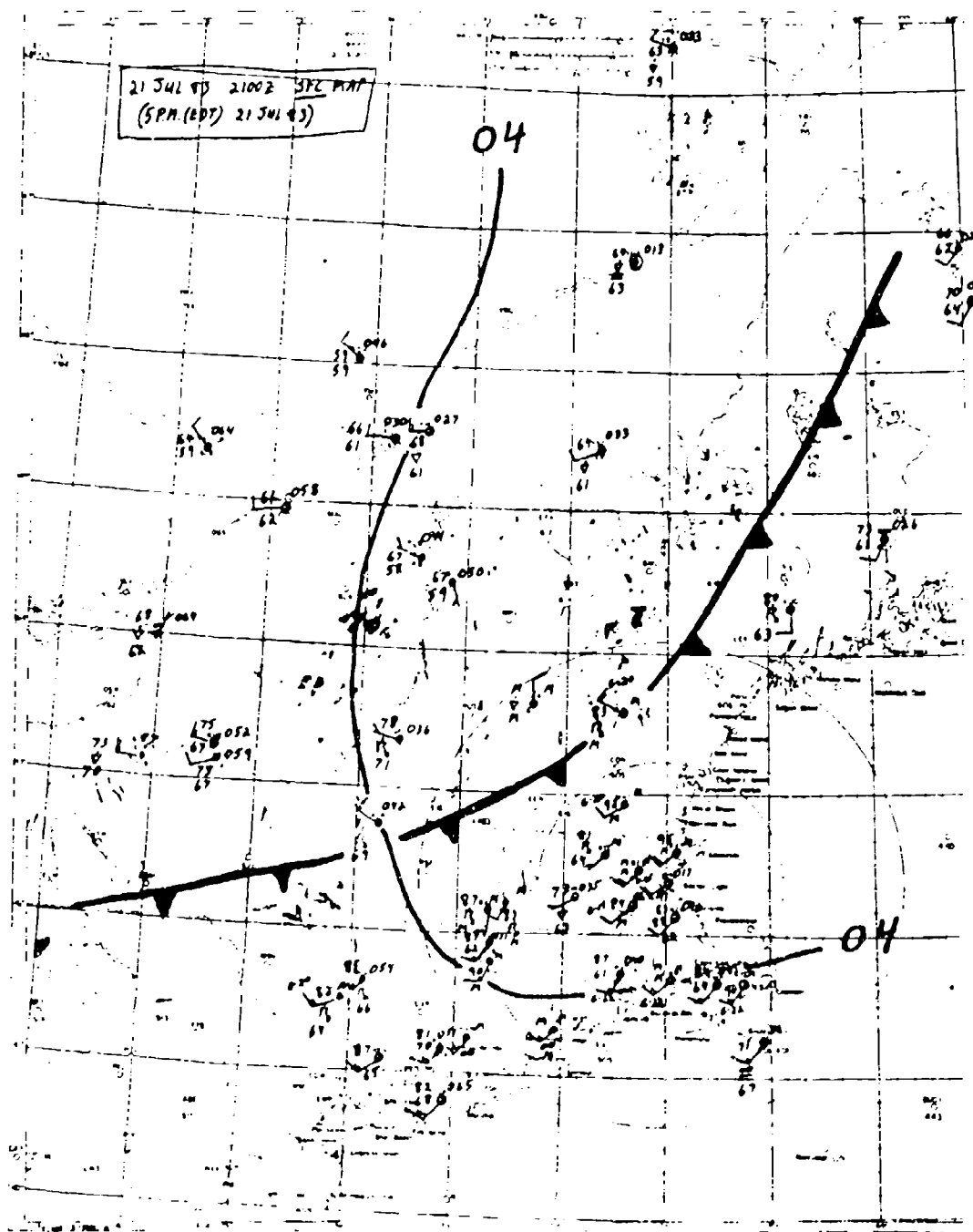


Fig. 3-1: Surface weather map showing New England area on 21 July 83 at 2100Z (5:00 P.M. (EDT)). The 04 line is the 1004 mb isobar.

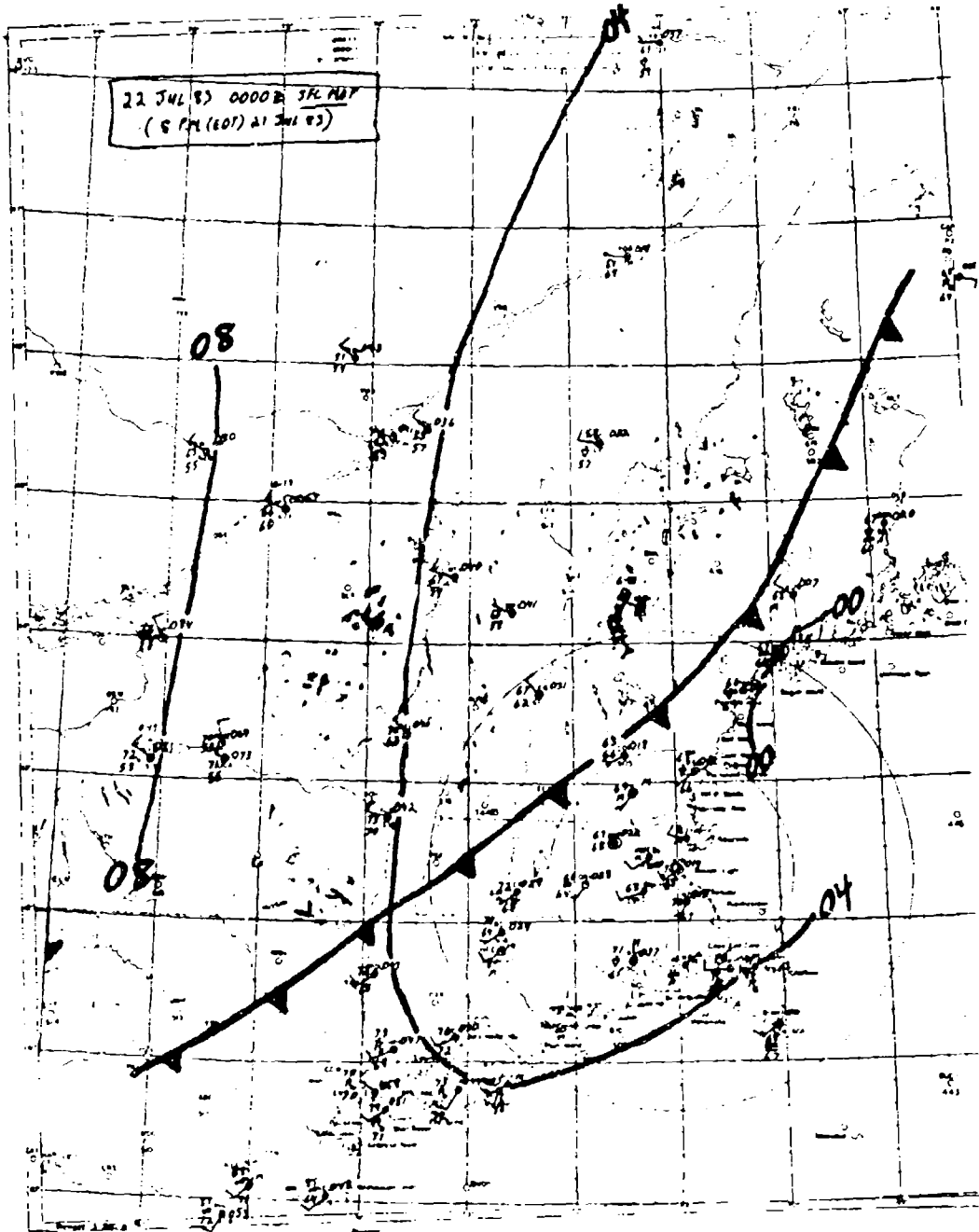


Fig. 3-2: Surface weather map showing New England area on 22 July 83 at 0000Z (8:00 P.M. (EDT) on 21 July 83). The 00, 04 and 08 lines refer to the 1000, 1004 and 1008 mb isobars respectively.

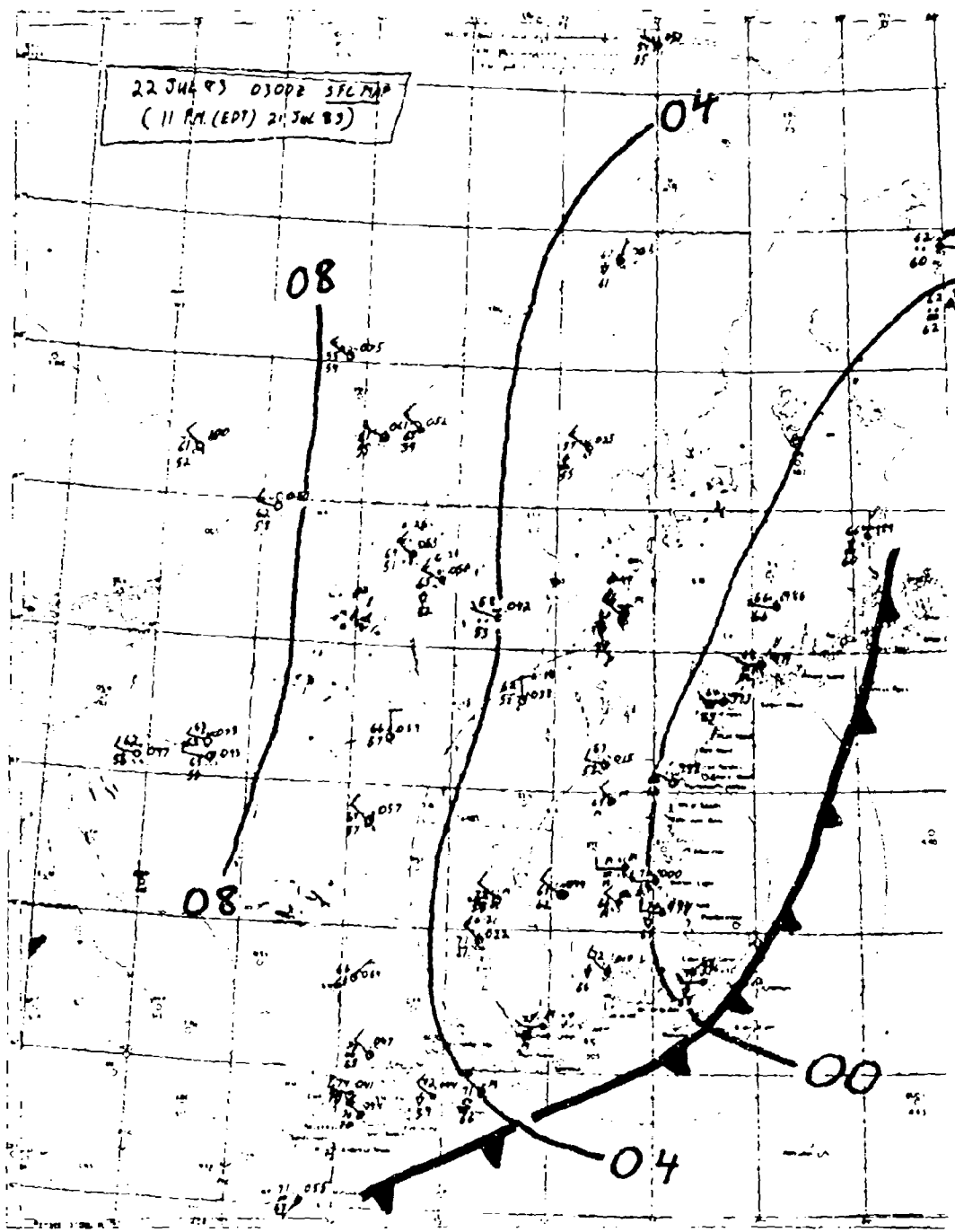


Fig. 3-3: Surface weather map showing New England area on 22 July 83 at 0300Z (11:00 P.M. (EDT) on 21 July 83). The 00, 04 and 08 lines refer to the 1000, 1004 and 1008 mb isobars respectively.

Abridged U. S. Model

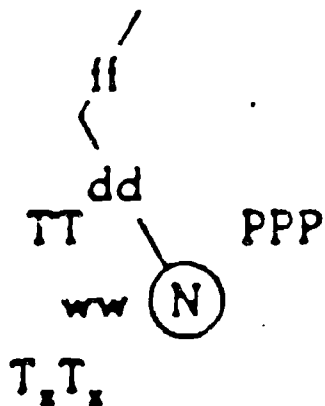


Fig. 3-4: Station model showing symbolic form of synoptic weather code. Represented codes are: 1) N-Sky Condition; 2) dd-Wind Direction; 3) ff-Wind Speed (kts); 4) TT-Temperature ($^{\circ}$ F); 5) ww-Present Weather Condition; 6) TxTx-Dew Point Temperature ($^{\circ}$ F); 7) PPP-Pressure (coded).



Fig. 3-5: Visible satellite image showing eastern half of U.S. for 22 July 83 at 12:30 P.M. (EDT).

responsible for bringing scattered rain and rain showers to the Hanscom area early in the day which was then followed by mostly cloudy conditions with very strong northerly winds and temperatures that were unseasonably cool for that time of year.

C. Satellite Data

The GOES (Geostationary Operational Environmental Satellite) imagery shows the view of the Earth and its accompanying cloud cover from a distance of more than 19,000 nautical miles above the earth's surface. With the assistance of the Air Force Geophysical Laboratory's (AFGL's) Satellite Meteorology Branch, we were able to acquire the GOES imagery, with a resolution of 2 km, for the time period involving the outbreak of convection which occurred over the Northeastern U.S. on July 21, 1983.

A sequence of visible satellite images encompassing the time interval between 11:00 a.m. and 4:30 p.m. (EDT) on July 21 are shown in Figures 3-6 through 3-17 respectively. At 11:00 a.m., Figure 3-6 shows most of New England cloud free with the exception of northern and eastern Maine and northeastern Vermont. Temperatures continued to climb in the cloud free areas. The convective activity at this time appeared well to the north of Lake Ontario and also in south-central Quebec Province. Also, a convective area showed up well, over the waters to the south of Cape Cod. This area of convection in the Atlantic posed no threat to New England. By 11:30 a.m. some of the clouds began to dissipate over Maine, and the convection to the north of Lake Ontario moved southeastward. By noon (Fig. 3-8), the satellite imagery showed the early development of clouds over the hills of Vermont, New York and western Massachusetts. One hour later (Fig. 3-10), the convective clouds from Canada began to spread into up-state New York and northern Vermont. By 1:30, convective clouds developed throughout much of New York state and the northern half of Vermont. This area of convection developed into strong thunderstorm cells and moved southeastward, affecting western Massachusetts by mid-afternoon (approximately 3:30 p.m. (Fig. 3-15)). By late afternoon (Fig. 3-17), these thunderstorms approached southern New England. At this time (4:30 p.m.), the surface cold front was in a position stretching northeast to southwest through central New England.

D. Mesonet Data

The mesonet data for the thirteen stations transmitting on July 21 and 22 have been plotted and are presented in Figures 3-19 through 3-31. As discussed in Chapter II, the data were averaged for 2.5 minutes out of every 3, giving 20 data points per hour. Figure 3-18 is a map showing the relative locations of the mesonet stations and their 3-letter identifiers. The other stations in the network that are not included were either not yet set up to transmit data or their transmissions were faulty and never received by the satellite.



Fig. 3-6: VISIBLE SATELLITE IMAGE - 21 JULY 83, 11:00 A.M. (1500 GMT)



Fig. 3-7: VISIBLE SATELLITE IMAGE - 21 JULY 83, 11:30 A.M. (1530 GMT)



Fig. 3-8: VISIBLE SATELLITE IMAGE - 21 JULY 83, 12 NOON (1600 GMT)



Fig. 3-9: VISIBLE SATELLITE IMAGE - 21 JULY 83, 12:30 P.M. (1630 GMT)



Fig. 3-10: VISIBLE SATELLITE IMAGE - 21 JULY 83, 1:00 P.M. (1700 GMT)



Fig. 3-11: VISIBLE SATELLITE IMAGE - 21 JULY 83, 1:30 P.M. (1730 GMT)



Fig. 3-12: VISIBLE SATELLITE IMAGE - 21 JULY 83, 2:00 P.M. (1800 GMT)



Fig. 3-13: VISIBLE SATELLITE IMAGE - 21 JULY 83, 2:30 P.M. (1830 GMT)



Fig. 3-14: VISIBLE SATELLITE IMAGE - 21 JULY 83, 3:00 P.M. (1900 GMT)



Fig. 3-15: VISIBLE SATELLITE IMAGE - 21 JULY 83, 3:30 P.M. (1930 GMT)



Fig. 3-16: VISIBLE SATELLITE IMAGE - 21 JULY 83, 4:00 P.M. (2000 GMT)



Fig. 3-17: VISIBLE SATELLITE IMAGE - 21 JULY 83, 4:30 P.M. (2030 GMT)

1. Explanation of Figures

Each figure consists of two plots, one for each day. The time is Greenwich Mean Time (subtract 4 hours for EDT). Each grid space in the horizontal direction represents one hour. The vertical units are labelled differently for each variable. The name of the variable and the units that apply to the label are printed under the individual graphs. Since there is not always enough space to plot the full range of a particular variable, we have used a "wrap around" scale. Thus, when the trace goes off the bottom of the scale it reappears at the top. The scale from then on should be interpreted so that the top most line is equal to the lowest labelled line, and the lower lines are still lower by increments equal to those originally set. In figure 3-19 the pressure on 21 July wraps around at 1008 millibars and falls to just below 1002 millibars between 2000 and 2100 hours. The curve can also wrap around by going off the top of the scale as it does with the temperature in that same figure. Notice that the temperature at AFC on 21 July peaked at about 33 degrees C.

The top of each graph is labelled with the three letter identifier for that station. The date is printed at the right and the satellite transmission identification code is printed at the left. The variables presented are battery voltage, pressure in millibars, temperature in degrees Celsius, relative humidity in percent, wind speed in meters per second and wind direction in degrees with north at 0 and east at 90 degrees.

2. Features of the Data

There are four main features of this 48 hour period to look for in the mesonet data:

<u>FEATURE</u>	<u>EDT</u>	<u>GMT</u>
1. Wind shift from south to west-southwest	7-9 am	11-13, 21 July
2. Thunderstorm moved through network	6-7 pm	22-23, 21 July
3. Cold front passed through network	10 pm-mid.	2-4, 22 July
4. Low developed and deepened off coast	8 am-noon	12-14, 22 July

The first feature is manifested simply by a shift in the wind direction from 180 to about 250 degrees. The thunderstorm moving through a network is evidenced by the sharp rise and gradual fall in pressure, and a peak in the wind speed trace. The cold frontal passage is indicated by a continued fall followed by a levelling out in the pressure field and a shift in wind direction from 270 to 315 degrees. Instead of immediately beginning to rise again as the pressure will often do after the passage of a cold front, it continued to gradually decrease under the influence of the surface low

pressure area off-shore. This low is also indicated by the strong increase in wind speed, the shift in wind direction from 315 to 355 degrees, the increase in relative humidity and a drop in the already unseasonably cool temperatures.

3. Discussion of Individual Station Data

AFC - Figure 3-19 - This station was probably the most reliable source of data and still, three transmissions were missed on 21 July. The 30 minutes of data preceding the thunderstorm passage are missing but the decline in pressure and wind speed are visible. Notice that the winds were a steady 10-12 m/s (25 mph) from 11 am to 4 pm on the 22nd when the winds were from due north.

LAW - Figure 3-20 - This station has perhaps the clearest signatures of all four significant weather features, even though the anemometer was reading only about half of what it should have been. Notice the sharp spike in the pressure and wind speed associated with the thunderstorm passage. Also notice that after the cold frontal passage the pressure actually did begin to rise but began to fall rapidly thereafter under the influence of the coastal low.

CON - Figure 3-21 - This station had so many problems it is difficult to tell how much, if any, of the data is valid. However, features 2 - 4 do appear to be present. The spurious spikes in the pressure and wind direction fields occur exactly at the time of transmission but are otherwise unexplained. This anemometer, like that at LAW, is also reading too low, but when it does read above 2 m/s the wind direction appears to return to normal. The spikes in the temperature field are due to the erroneous addition or subtraction of 256 digital counts to the data average, but this also occurs only at transmission times and only when the temperature is above about 25 degrees C.

DUD - Figure 3-22 - This station exhibited many of the same problems as CON did. While a total of only three transmissions are missing, two of them occurred during the interesting part of the data. These same three transmissions are missing in quite a few of the stations' reports (2200 GMT on 21 July and 330, 1300 GMT on 22 July).

VER - Figure 3-23 - This station's data was also fairly reliable for most of the summer. In this figure as well, two significant data transmissions are missing. Notice how the battery voltage rises during the peak sunlight hours when the solar panel output is the greatest.

NUB - Figure 3-24 - This station had quite a few missed transmissions and a bad wind speed sensor, but otherwise the data was fairly good. As usual, the data lost was for the most meteorologically interesting times.

NAG - Figure 3-25 - A large amount of data was lost due to a faulty transmitter on 21 July from about noon to 6 pm EDT. Notice, however, that the thunderstorm signature was just visible and the features occurring on July 22 were recorded.

JWL - Figure 3-26 - This station, like NAG, also lost data during the evening hours of the 21st. The scalloped pressure trace is still unexplained, except to notice that the dips occur at the transmit times. This station perhaps best captured the sudden 9 am (13 GMT, 22 July) drop in temperature and increase in relative humidity when the wind shifted around to the north as the low pressure area moved off-shore.

PIG - Figure 3-27 - This station exhibited many of the same problems mentioned for the other stations. The anemometer was reading far too low, and was perhaps being mechanically prevented from turning freely. The wind direction data for this station also looks very suspicious.

VAL - Figure 3-28 - The most obvious problem with this station was the barometric pressure which varied wildly between extreme limits. None of the pressure data are meaningful. Quite a few transmissions were missed, some of them at significant times. The temperature and relative humidity data do appear to have spurious spikes and large variations that are probably unreal.

GGG - Figure 3-29 - Although this station transmitted data fairly reliably, it did exhibit many of the same problems that the other stations did.

FSK - Figure 3-30 - This station had a faulty transmitter which managed to work about 2 or 3 times each day. The data that did get reported are basically meaningless.

AWD - Figure 3-31 - No data at all were transmitted on the 21st of July for this station. On the 22nd some data of questionable value was transmitted.

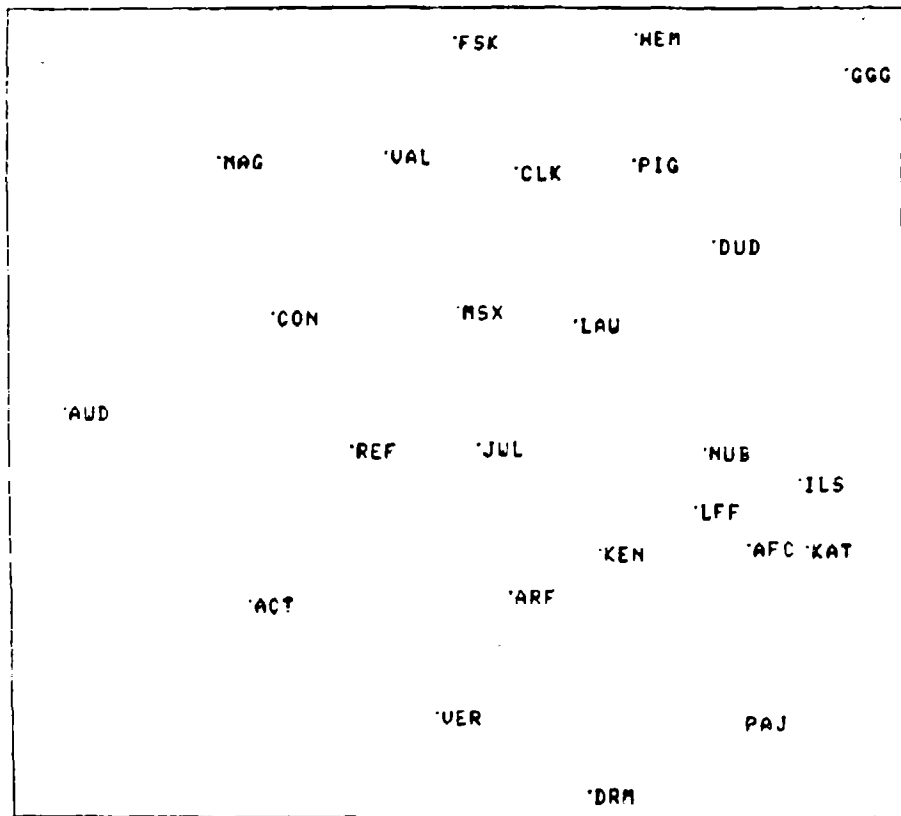
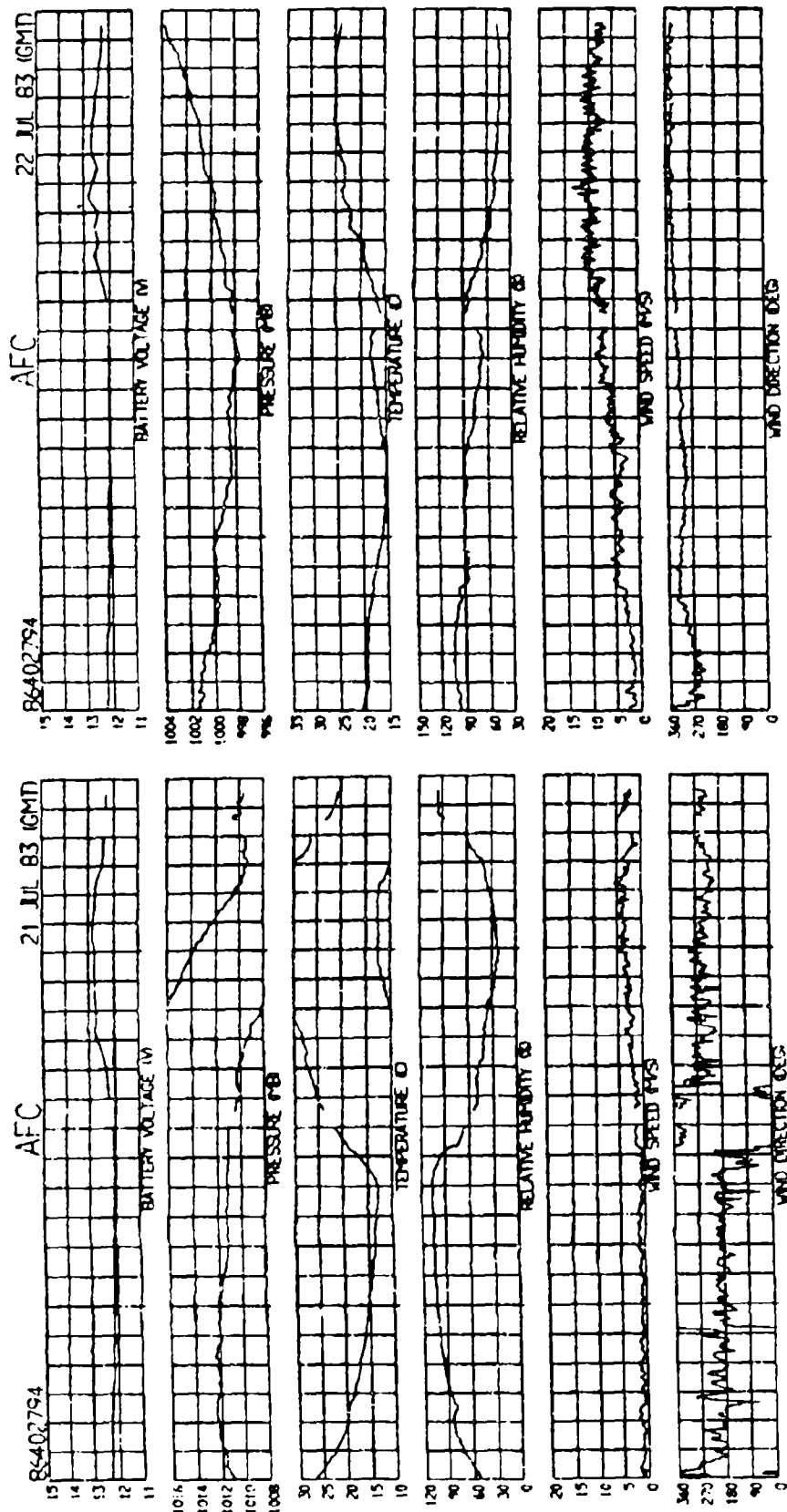


Fig. 3-18: Map of weather stations showing relative locations and 3-letter identifying names. Refer to Fig. 2-3 for geographical location.



NO PRECIP DATA

Fig. 3-19: Mesonet data - AFC

NO PRECIP DATA

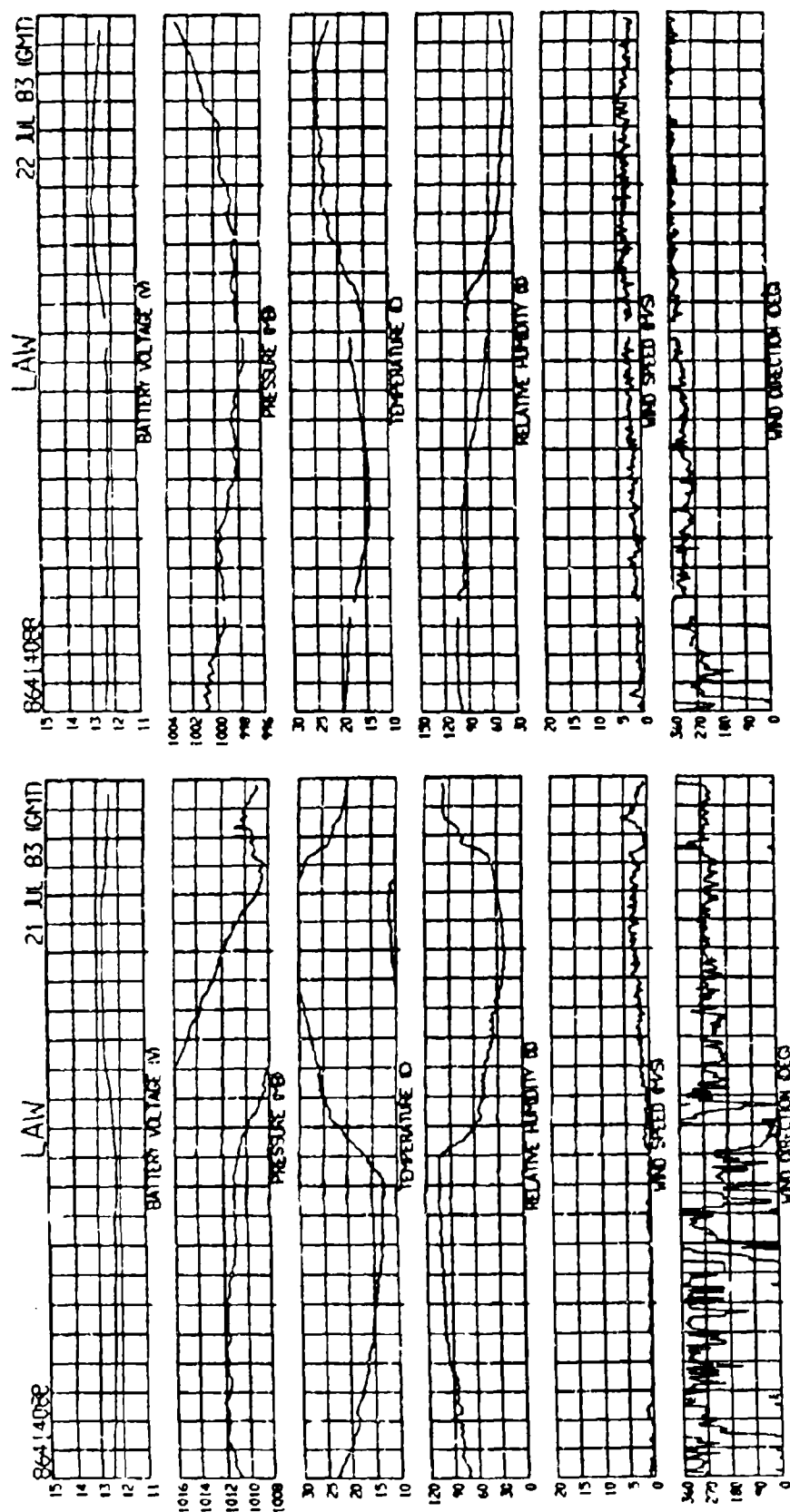
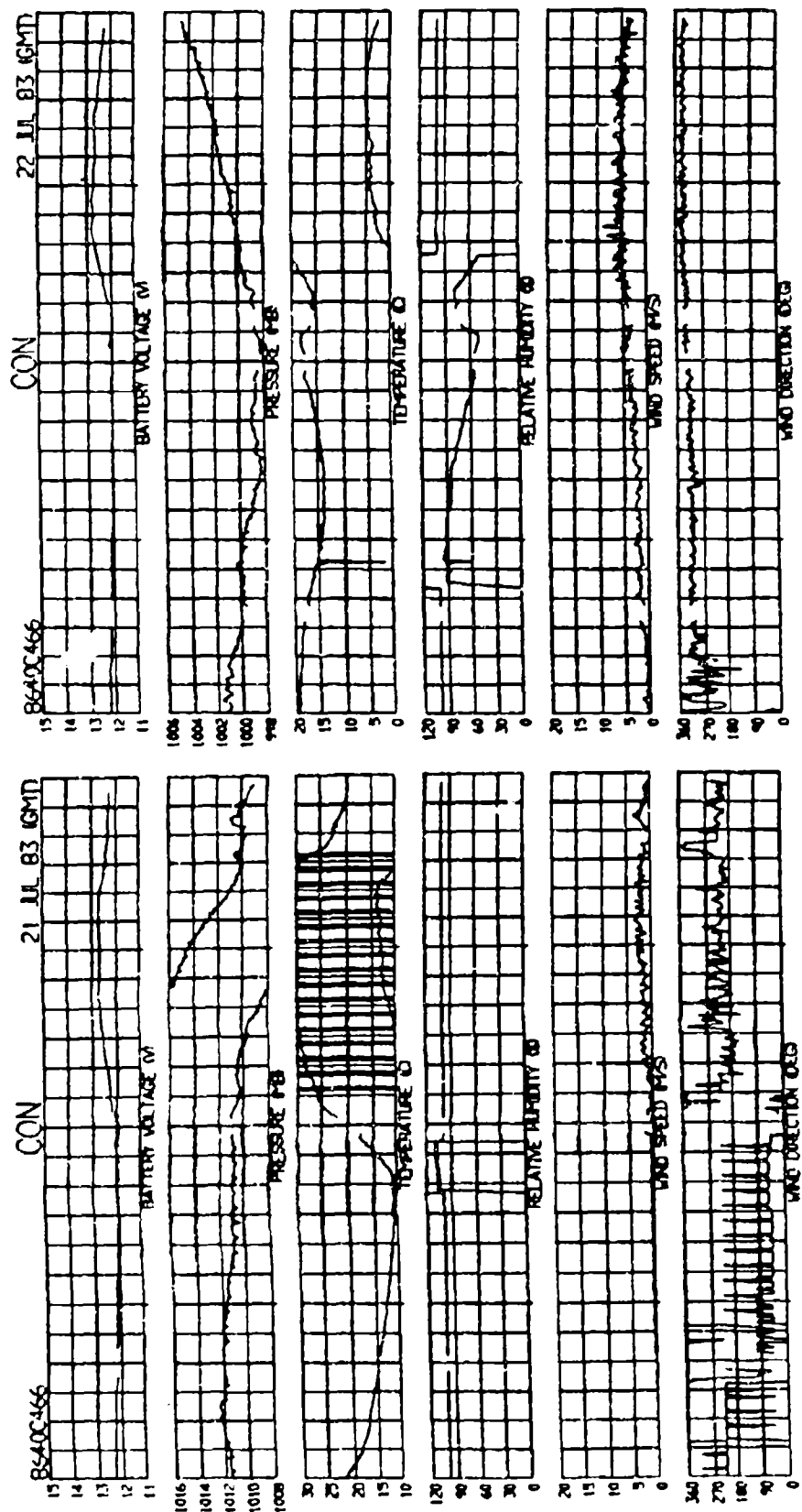


Fig. 3-20: Mesonet data - LAW

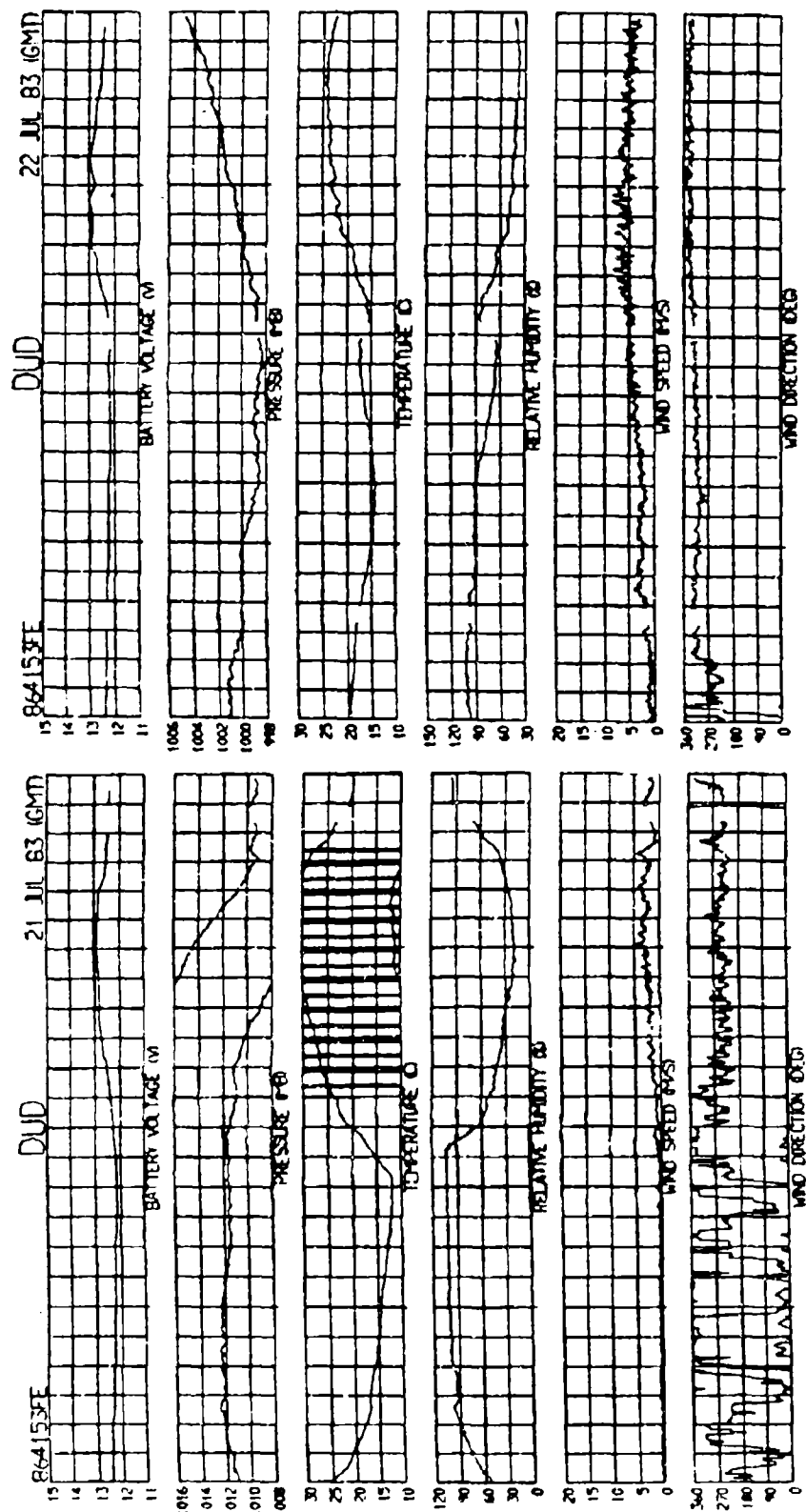
NO PRECIP DATA

NO PRECIP DATA



NO PRECIP DATA

FIG. 3-21: Mesonet data - CON



NO PRECIP DATA

Fig. 3-22: Mesonet data - DUD

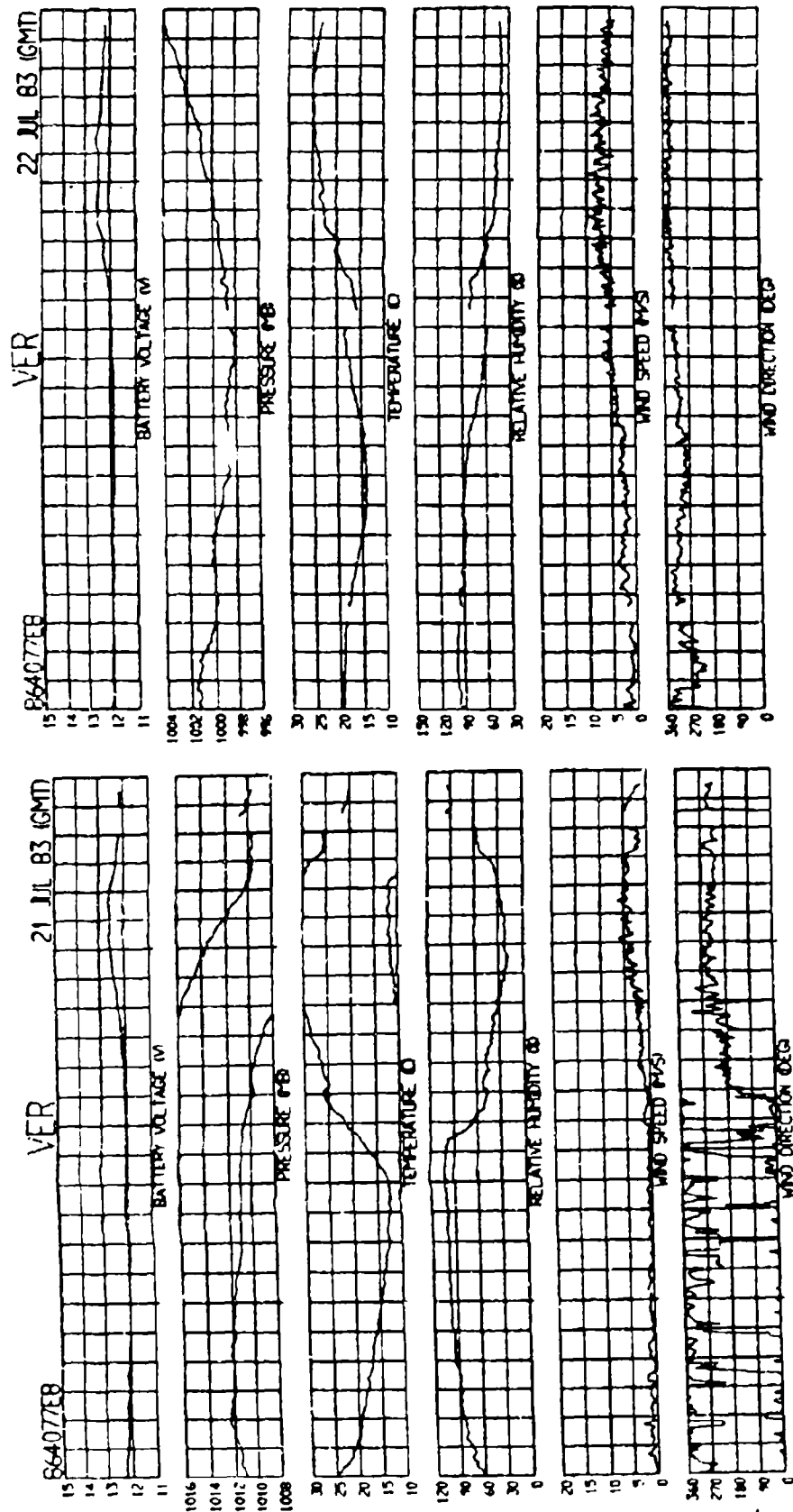


Fig. 3-23: Mesonet data - VER

NO FRECIR DAI

NC PRECIP DATA

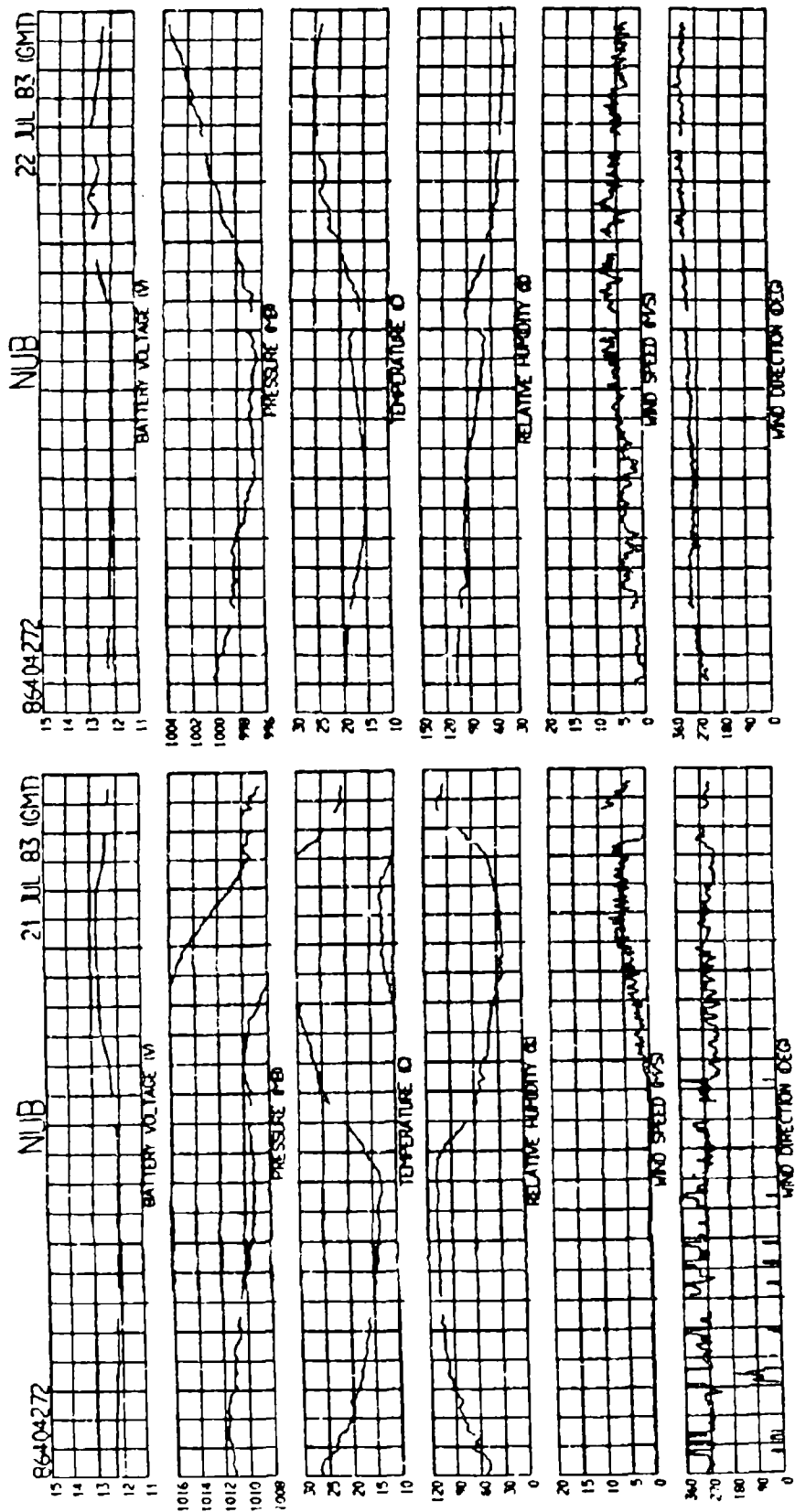
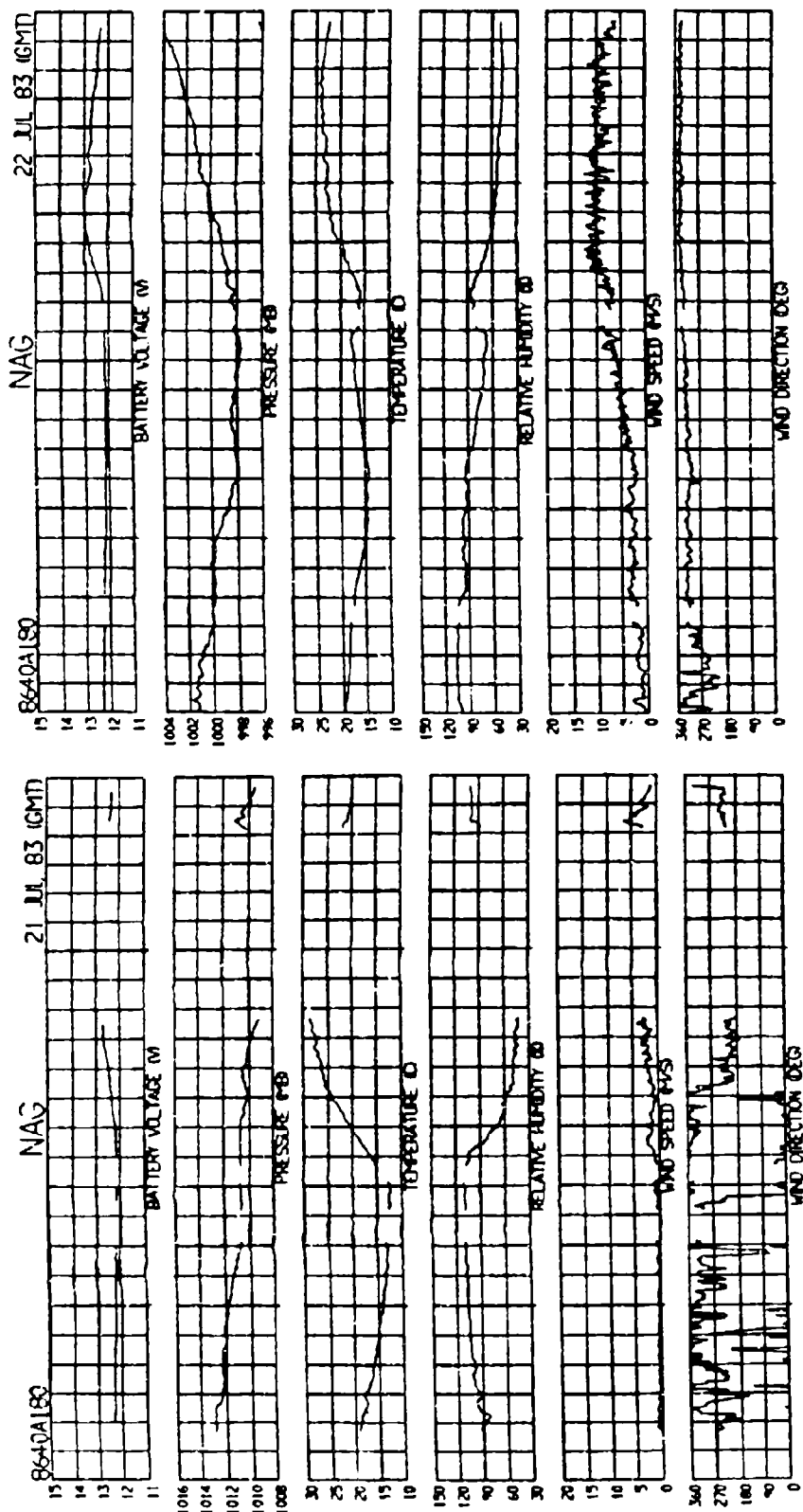
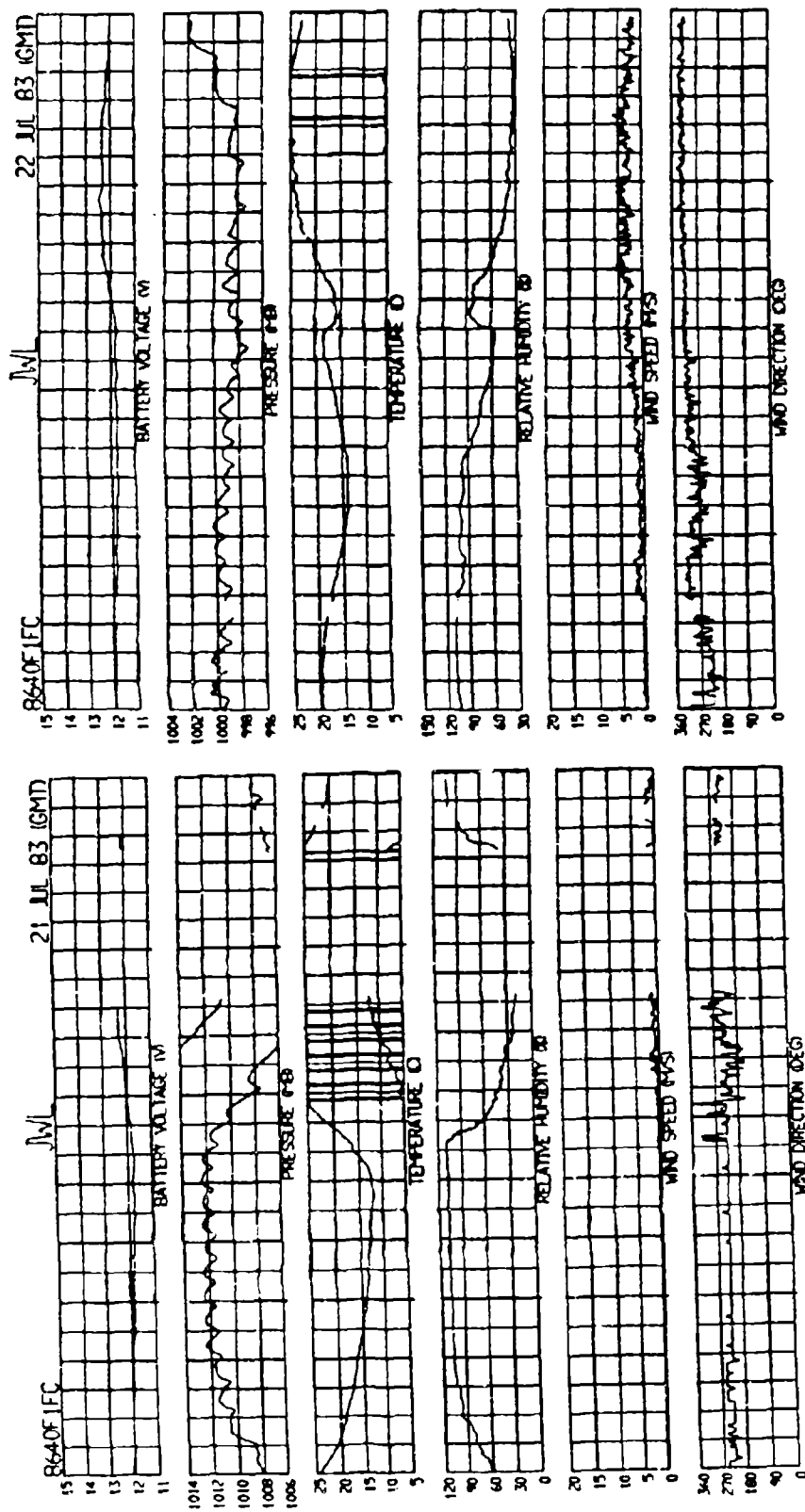


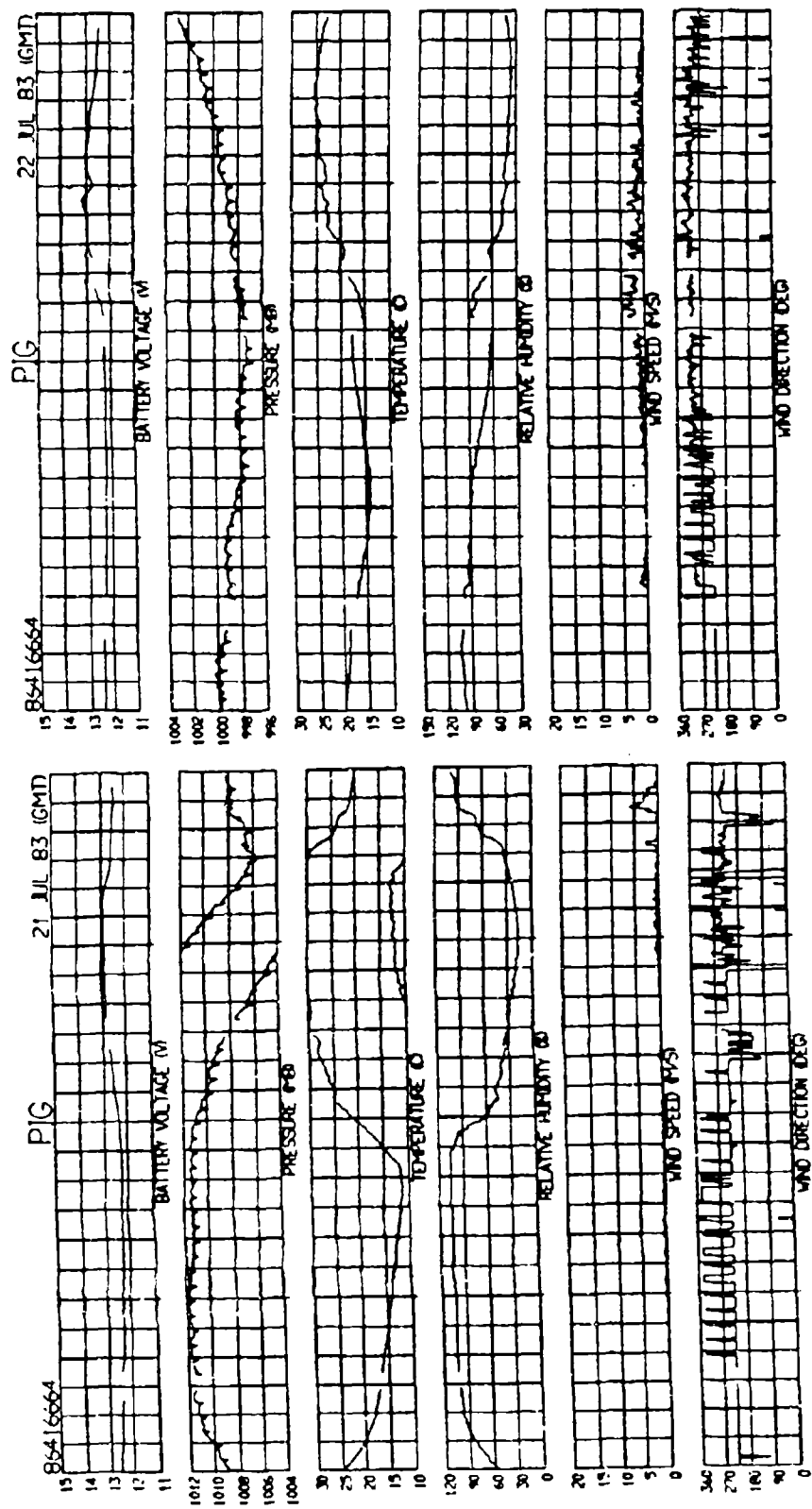
FIG. 3-24: Mesonet data - NUB



NO PRECIP DATA

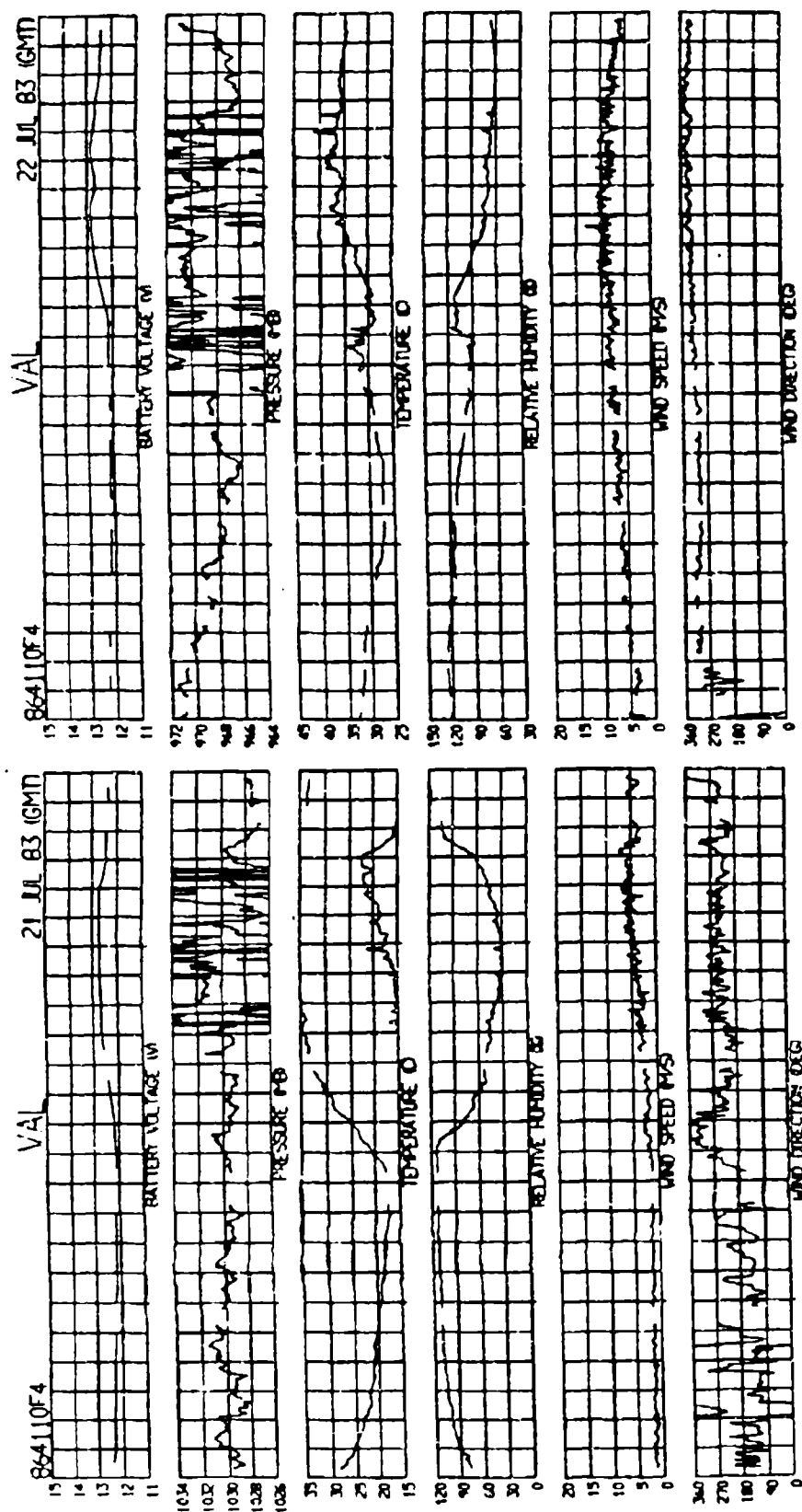
F18. 3-25: Mesonet data - NAG





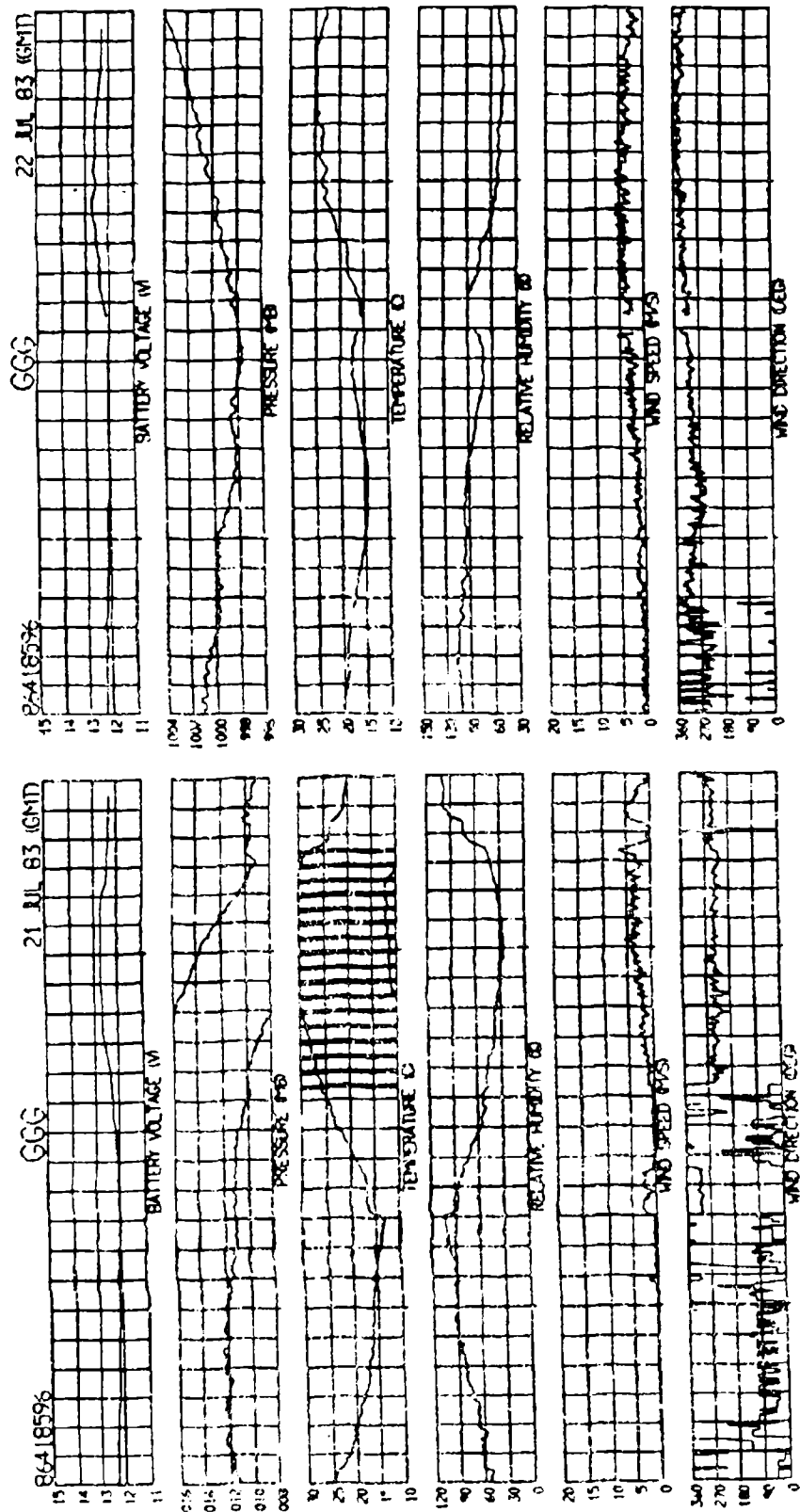
NO PRECIP DATA

Fig. 3-27: Mesonet data - PIG



NO PRECIP DATA

Fig. 3-28: Mesonet data - VAL.



NO PRECIP DATA

Fig. 3-29: Mesonet data - CCC

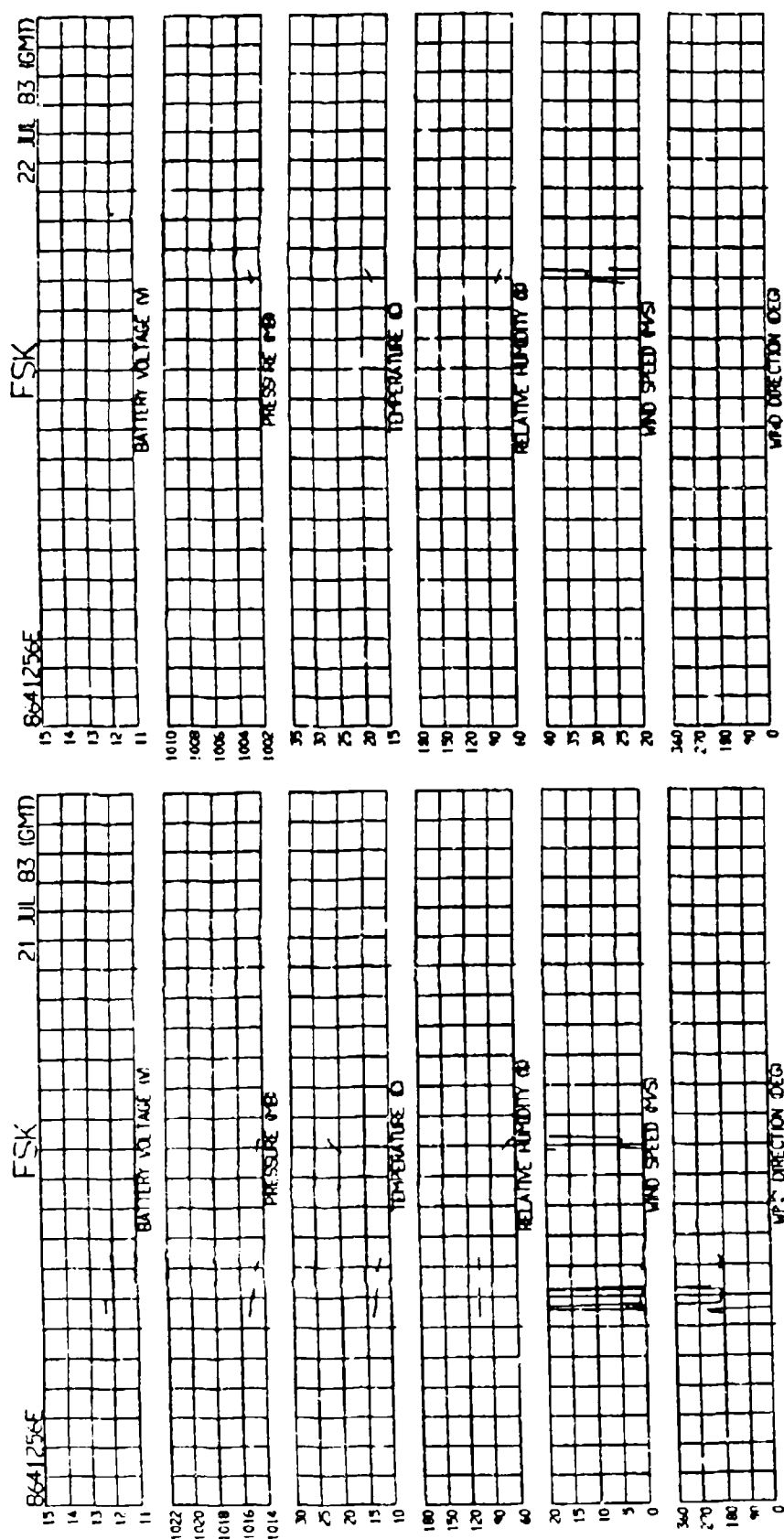
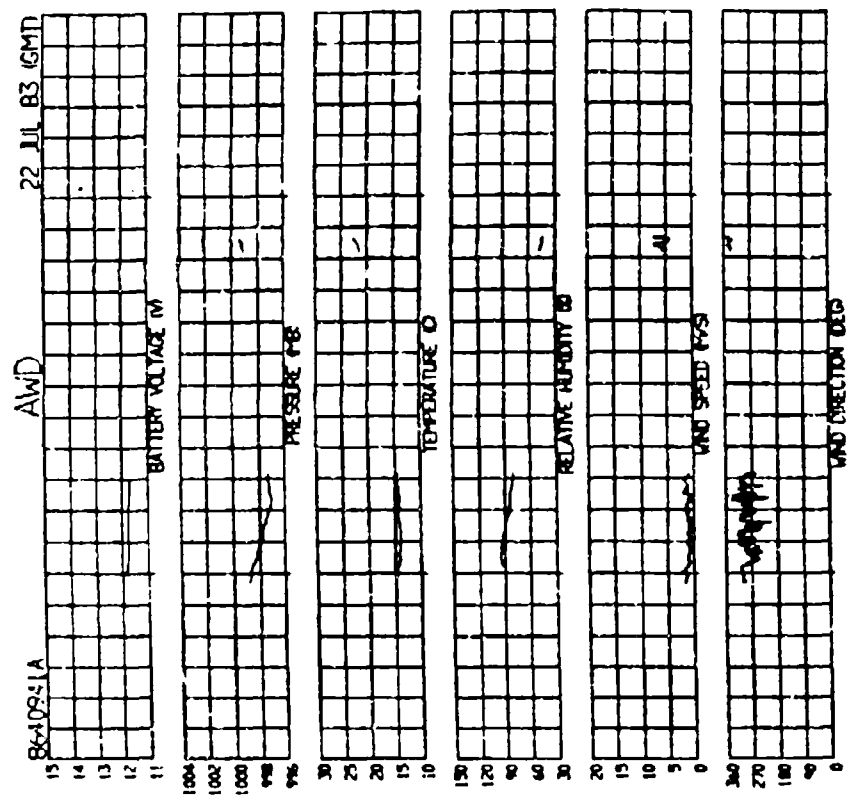


Fig. 3-30: Mesonet data - FSK



NO DATA

NO PRECIP DATA

Fig. 3-31: Mesonet data - Awd

E. Doppler Radar Data

Doppler weather radar data was collected during the day and early evening on 21 July 1983 with the MIT radar. The storm situation shown in Fig. 3-32 occurred at (a.) 6:51 pm EDT and (b.) 7:00 pm, approximately 20 and 30 minutes, respectively, after the passage of the thunderstorm ("feature 2" in the mesonet data, discussed in section D). The time displayed in the figure is Eastern Standard Time, five hours behind Greenwich Mean Time.

There is a cursor or marker in the lower part of each figure between the first and second range rings. The location in both spherical and Cartesian coordinates of the cursor, relative to the radar, is given in the lower right corner of the figures. "X" refers to kilometers east, "Y" km north, "Z" km up, "R" km range, "A" degrees azimuth, and "E" elevation angle, also in degrees, of the cursor at its displayed location. Notice how the storm cell near the cursor moved in the 9 minutes between snapshots (the cursor is in the same position in both Figs. 3-32 (a.) and (b.); the height is different because the data from slightly different elevation angles are presented). The storm motion was primarily from west to east with a small component of motion from south to north.

The bright areas of high reflectivity represent the heavy rainfall areas. The storm that is between Hanscom Field and the MIT radar (sites identified in Fig. 3-32 (c)) is basically the same cell that came through the weather station network half an hour earlier.

F. Damage Reports*

In Massachusetts the areas strongest hit by the thunderstorms on July 21, 1983 were the communities which bordered New Hampshire. However, the rest of Massachusetts was not exempt from the effects of this severe weather. Reports first came in from communities in the western part of the state at about 4:45 (EDT). Some of these western Massachusetts counties (S. Amherst, Hadley, Spencer and East Brookfield) reported funnel cloud sightings. There were also reports of several large trees being snapped off and others that were twisted out of the ground.

Prompted by the reports of funnel clouds in these counties, a tornado warning was issued in Worcester county, but there were no confirmed reports of any tornadoes. Now, further to the east during the late afternoon and early evening hours, wind gusts were estimated to have reached 70-80 MPH in the Dracut, Methuen, Leominster and Haverhill communities. These winds blew down many trees and tree limbs which caused injuries to several persons. Automobile windshields which were smashed by the falling tree limbs were reported in Leominster and Dracut. Power was knocked out in the area, including all of Haverhill, and the roof was blown off a country club in Methuen. In Salisbury, between 6:00 and 6:30 EDT, thunderstorm winds which gusted up to an estimated 70-80 MPH ripped through the campground at the state reservation over-turning two trailers and leveling about 30 tents. Six persons were injured by flying debris.

*Damage reports were taken out of the July 1983 issue of "Storm Data" which is published by the National Oceanic and Atmospheric Administration and is compiled from information received at the National Climatic Data Center.

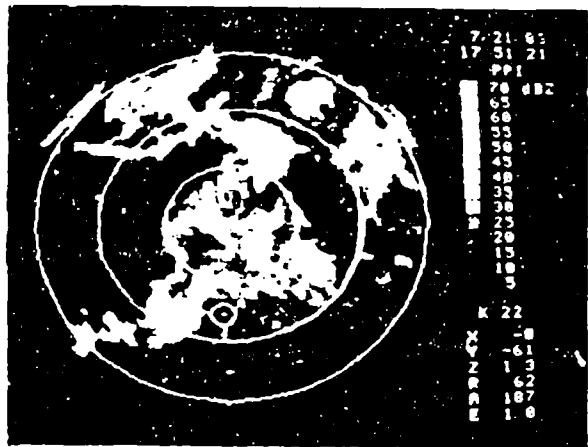


Fig. 3-32 (a): MIT Radar reflectivity, 17:51 EST.

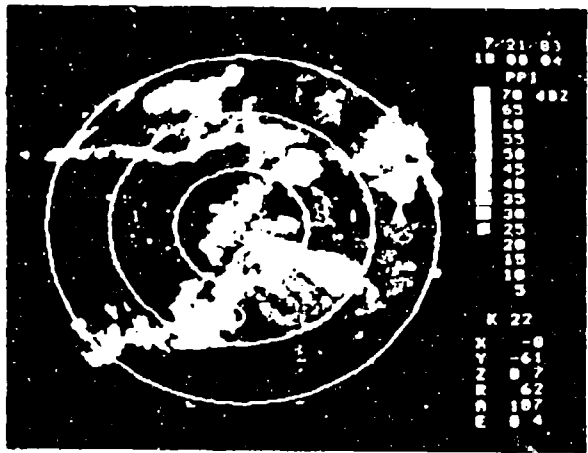


Fig. 3-32 (b): MIT Radar reflectivity, 18:00 EST.

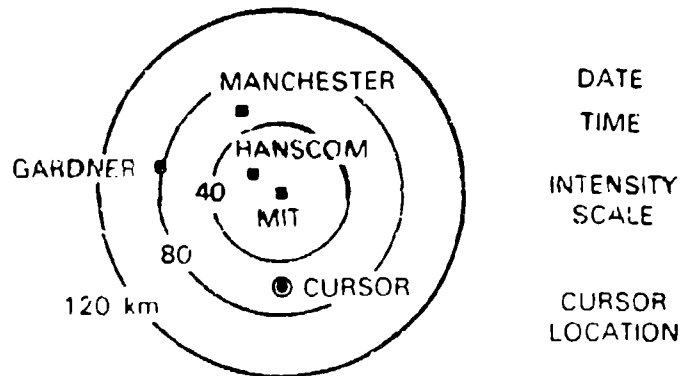


Fig. 3-32 (c): Key to radar display.

IV. CONCLUSIONS

A. Upgrading Mesonet Equipment

The primary objectives of operating a mesonet of automatic weather stations as part of a Doppler radar data collection experiment are: 1) to provide confirmation of low altitude wind shear events detected in the Doppler data and 2) to provide an indication of otherwise undetected wind shear events. In order to achieve these objectives, measurements must be made that are consistent with the spatial and temporal scales of microbursts, the smallest and shortest lived of the known hazardous wind shears. These objectives also obviously require that the equipment be operational at least 95% of the time. Unfortunately, meeting these objectives will require a rather costly upgrade of the mesonet equipment.

1. Temporal Resolution

The importance of fine temporal resolution in measuring microbursts is illustrated in Fig. 4-1, which depicts the wind speed trace of a microburst that occurred at Stapleton International Airport during the Joint Airport Weather Studies (JAWS) experiment in May of 1982. Both the actual one minute averaged data collected by their Station 4 and simulated three minute averaged data, similar to that we collected during our experiment, are shown. By lengthening the averaging period, the maximum winds detected were reduced by 20% in the most favorable case (when they fell exactly in the middle of the 3 minute period). Also, fluctuations in the wind speed have been completely erased, and the transition from low to high winds appears smooth and steady rather than impulsive. Thus, one minute averages are the most "coarse" surface wind measurements that are acceptable. As discussed in Chapter II, our electronic equipment is suitable only for averaging periods greater than two minutes. We therefore conclude that this equipment is inadequate for continued use in measuring microburst wind shear.

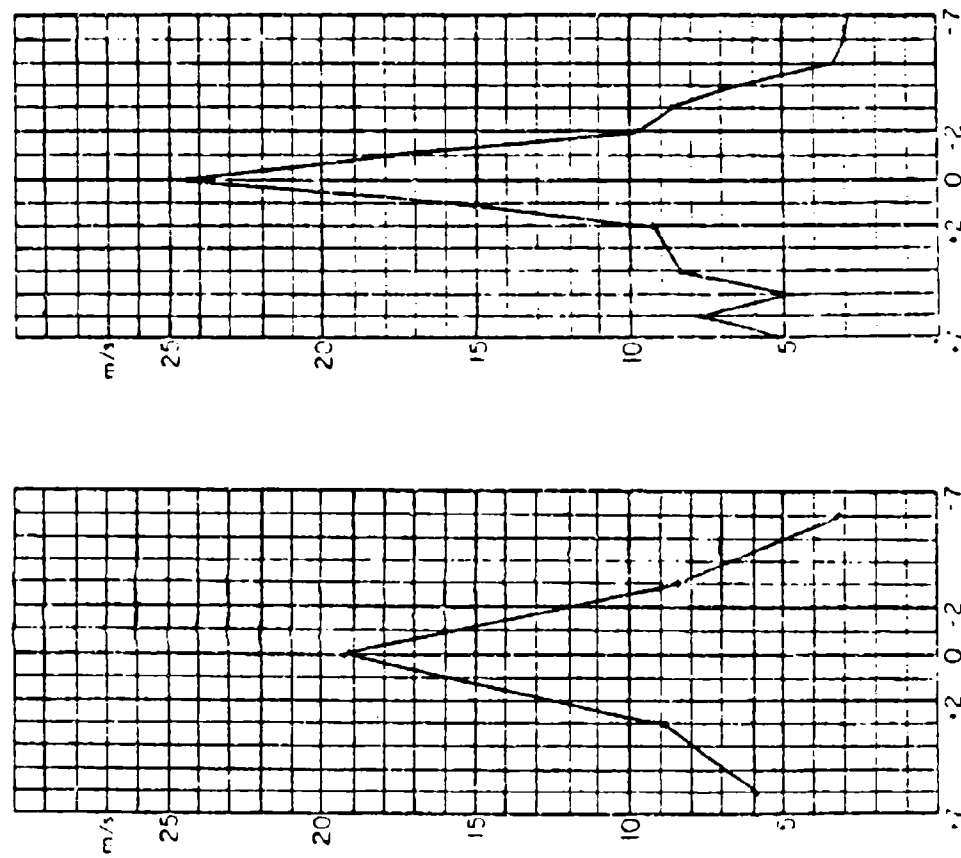
2. Operational Reliability

Meeting the objectives of detecting and confirming wind shear events will require operationally reliable equipment and, if possible, very little post real-time processing. Unfortunately, these are features that the summer 1983 mesonet system lacked.

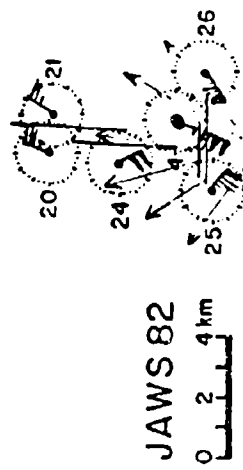
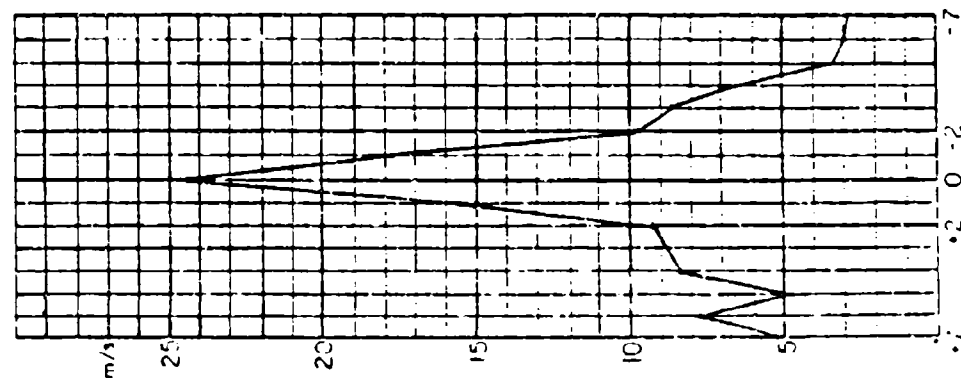
Of the 23 stations operating during July and August only 5 were operational 95% or more of the time. The problems that plagued the other stations ranged from still unexplained intermittencies, to corrosion on the motherboard due to exposure and age, to manufacturer specified modifications that were never made in the Handar Data Collection Platform, to spikes in the data of stations programmed to transmit at times that were integer multiples of the averaging interval. Some of the problems were fixed but required a technician's attention on a nearly full-time basis. Fixing other problems would have required hardware modifications.

19 MAY 1983 12:56 MICROBURST STATION 4

SIMULATED 3 MIN AVG



ACTUAL 1 MIN AVG



STAPLETON INTERNATIONAL
AIRPORT
DENVER, COLORADO

Fig. 4-1: Comparison of actual 1-minute averaged wind speed data for 15 minutes during which a microburst occurred, with simulated 3-minute averaged data for the same time period.

The data relayed by satellite consisted of digital counts for each sensor plus two higher order bits which determined the additive constant of 0, 256, 512, or 768. The sum was scaled and offset, plus multiplied by a fraction which compensated for the difference between the actual averaging interval and that set on the motherboard, as part of the conversion to engineering units. While this conversion was fairly straightforward with the aid of a computer, the user could not instantly see that a problem had occurred by simply glancing at the transmitted data.

When considering system reliability, the methods of data collection and archival must also be examined. During the summer of 1983 we explored two options: 1) dissemination of the data via 1200 baud telephone communications with the NOAA-NESDIS Data Collection Service, and 2) reception of the data on 1600 bpi magnetic tape, collected and recorded by a private corporation with their own GOES ground station. The latter proved to be nearly 100% reliable and required no Lincoln staff member's attention but was expensive while the former required our daily attention and provided an incomplete data set due to NESDIS system crashes and downtime but was otherwise free of charge.

In conclusion, the poor reliability of the electronic equipment and the NESDIS data collection system prevented a large part of the desired data from being obtained.

V. RECOMMENDATIONS

A. Equipment Upgrades

The mechanical structure which supports the electronics and sensors is very well designed and should continue to be used. The sensors themselves are reliable and should also continue to be used. The Data Collection Platforms would have to be sent back to the manufacturer to have all of the modifications made to bring them up to date before they could be used again. Even if this were done, since these particular DCPs must be used with an electronics package, extensive refurbishment or replacement of the motherboards would also have to take place.

We recommend that new Data Collection Platforms be purchased that will eliminate the need for a separate motherboard, perform the calculations internally to convert the data to engineering units before transmission, allow one minute averages, use an approved binary transmission code that will allow us to send three times as much data per transmission, and will report the DCP status with each transmission. We also recommend soliciting bids from private firms for the job of downlinking and archiving our data.

Although the sensors themselves are still good, we further recommend that the calibration of the sensors be handled by technicians at Lincoln Laboratory. This is the only way that we can assure the quality of calibration necessary for our successful data collection.

B. Future Measurements

By June of 1984 we will have assembled a Doppler weather radar testbed that will be taken first to Olive Branch, Mississippi (just southeast of Memphis, TN) and then to other sites in approximately 6 month intervals, to collect data on thunderstorms and severe low altitude wind shear. This data will be of use in learning to automatically detect and warn the aviation community against weather hazards. The refurbished weather stations will accompany the testbed to make simultaneous measurements of the surface meteorological variables during thunderstorms. They will serve as a principal data source for assessing the low altitude wind shear detection performance of the radar.

REFERENCES

1. Wilson, J. and R. Roberts, 1983: Evaluation of Doppler radar for airport wind shear detection. Preprints, Twenty-first Conference on Radar Meteorology, Edmonton, Alberta, 616-623.
2. Fujita, T. T., 1983: Analysis of storm-cell hazards to aviation as related to terminal Doppler radar siting and update rate. SMRP Research Paper No. 204, University of Chicago.
3. Fujita, T. T., 1983: Microburst wind shear at New Orleans International Airport, Kenner, Louisiana on July 9, 1982. SMRP Research Paper 199, University of Chicago.

APPENDIX A

Summary of Weather Events and Collected Data

During the Summer Storm Project of 1983, data for twelve various storm cases were collected. Table A-1 lists the dates on which the data was collected as well as the weather situation that affected the local area within a 60 km radius of MIT in Cambridge. Meteorological information concerning each case was sought. Table A-2 shows the status of the meteorological data collection. This data set included: 1) Weather Summaries -- a short discussion of the weather situation; 2) Hourly Surface Reports; 3) Upper-Level Meteorological Charts; 4) Radiosondes - measurements of pressure, temperature and humidity in the vertical and 5) Satellite Imagery. Not mentioned in Table A-2 is that radar data (reflectivity, doppler velocity and spectrum width) was also collected for each case during this project interval.

TABLE A-1

<u>DATE</u>	<u>SYNOPTIC SITUATION</u>	<u>ASSOCIATED LOCAL WEATHER WITHIN 60 KM OF MIT</u>
14 June 83	Hot and humid air-flow	Scattered T-storms
15 June 83	Hot and humid air-flow	Scattered T-storms
5 July 83	Cold front advancing from the west	T-storms (some heavy)
9 July 83	Cold front advancing from the north	Mainly showers
18 July 83	Very hot and humid air-flow	Isolated heavy T-storms (LLWS verified)
21 July 83	Strong frontal zone approaching from north-west	Heavy T-storms (hail reported)
24 July 83	Surface trough approaching from the west	Rain and rain showers
1 Aug 83	Warm and very humid air-flow following warm frontal passage	Heavy T-storms (moving eastward to be in area by early evening)
4 Aug 83 a.m.	Warm and very moist southwesterly air-flow	Intense T-storm tracked eastward passing south of Boston (hail reported)
	p.m. Very warm and humid air-flow	Heavy T-storms moved eastward from south-central Mass. passing over Boston
6 Aug 83	Very hot and humid air-flow	Scattered convective activity during mid-late afternoon
12 Aug 83	Wintertime like pattern - low pressure moves eastward skirting the southern coast of New England	Rainy and windy

TABLE A-2

<u>Date</u>	<u>Weather Summary</u>	<u>Hourly SPC Reports</u>	<u>Upper-Level Charts</u>	<u>Radiosondes</u>	<u>Satellite Imagery</u>
14 June 83	C	C	C	NC	A
15 June 83	C	NC	C	C	A
5 July 83	C	C	C	C	A
9 July 83	C	C	C	C	NA
18 July 83	C	NC	C	C	A
21 July 83	C	C	C	C	A
24 July 83	C	C	C	C	NA
1 Aug 83	C	C	C	C	A
4 Aug 83	C	C	C	C	A
6 Aug 83	C	C	C	C	NA
12 Aug 83	C	NC	C	C	A

C = Complete

NC = Not Complete

A = Available

NA = Not Available

Hourly SPC reports cover regions of Northeast U.S. and Southeast Canada

APPENDIX B

Data Requests

In support of our investigations for the FAA, we have collected and will continue to collect Doppler weather radar data, instrumented aircraft data, and surface meteorological data during rain and thunderstorms. In some cases we have also archived NWS hourly surface data and GOES visible and IR data. We realize that our data sets are useful for meteorological and other scientific investigations and we welcome any requests for them. We do, however, ask that you do the following:

1. Request the data by contacting one of us at (617)863-5500

Marilyn Wolfson x3409
John DiStefano x3452
Barbara Gonsalves x3416

2. Provide blank magnetic tapes on which we can record your data. Data format descriptions will be provided.

3. Acknowledge the source of the data in any published reports by including an appropriate version of the following statement:

"The data used in this report was provided by the MIT Lincoln Laboratory under sponsorship from the Federal Aviation Administration."

4. Provide us with one copy of your publication.

Please do not hesitate to contact us if you have any problems or questions in using the data.